



HAL
open science

Mesozoic halokinesis and basement inheritance in the eastern Provence fold-thrust belt, SE France

N. Espurt, F. Wattellier, J. Philip, Jean-Claude Hippolyte, O Bellier, L. Bestani

► **To cite this version:**

N. Espurt, F. Wattellier, J. Philip, Jean-Claude Hippolyte, O Bellier, et al.. Mesozoic halokinesis and basement inheritance in the eastern Provence fold-thrust belt, SE France. *Tectonophysics*, 2019, 766, pp.60-80. 10.1016/j.tecto.2019.04.027 . hal-02324480

HAL Id: hal-02324480

<https://hal.science/hal-02324480>

Submitted on 7 Mar 2020

HAL is a multi-disciplinary open access archive for the deposit and dissemination of scientific research documents, whether they are published or not. The documents may come from teaching and research institutions in France or abroad, or from public or private research centers.

L'archive ouverte pluridisciplinaire **HAL**, est destinée au dépôt et à la diffusion de documents scientifiques de niveau recherche, publiés ou non, émanant des établissements d'enseignement et de recherche français ou étrangers, des laboratoires publics ou privés.

Mesozoic halokinesis and basement inheritance in the eastern Provence fold-thrust belt, SE France

N. Espurt^{1*}, F. Wattellier^{1,2}, J. Philip¹, J.-C. Hippolyte¹, O. Bellier¹, and L. Bestani^{1,3}

¹Aix Marseille Univ, CNRS, IRD, INRA, Coll France, CEREGE, Aix-en-Provence, France.

²Now at : FLODIM, 110 rue des rizières, Technoparc des grandes terres, 04100 Manosque, France.

³Now at : 47 rue Détrois, 33200 Bordeaux, France.

*Corresponding author

Abstract

The Provence Chain incorporated preexisting halokinetic and basement features which have played a key role in the structural evolution of the thrust systems. Field structural data, previously published geological maps and exploration well data have been used to interpret a new ~80 km-long balanced and restored cross section across the eastern Provence fold-thrust belt. The geological data and cross section construction suggest evidence for Mesozoic salt domes and minibasins embedded in the thin-skinned thrusts, and upper Paleozoic extensional structures transported on new thick-skinned thrusts. According to field data, pre-contractual palinspastic restoration suggests that salt domes and minibasins grew mainly during Rhaetian to upper Jurassic times and intermittently until the lower Santonian. Minibasins are mainly filled by carbonate systems associated with gravitational instabilities in minor normal faulting. Minibasin sinking into middle-upper Triassic evaporitic-carbonate succession has been mainly controlled by sediment loading. However, the initiation of salt movements might have been controlled by the initial geometry of the Triassic strata and probably extensional basement faulting. Preexisting salt structures have controlled thrust emplacements and their kinematics. Synorogenic deposits indicate a classical hinterland to foreland sequence of thrust inversion of the margin during the upper Cretaceous-Eocene Pyrenean-Provence compression.

Diapiric structures were mainly eroded during and after the Pyrenean-Provence compression then reactivated during Oligocene extension and Miocene to present-day Alpine compression. Cross section balancing shows a total horizontal shortening of 28.5 km related to the Pyrenean-Provence and Alpine compressions. The eastern Provence fold-thrust belt integrates preexisting halokinetic folding which can be misinterpreted as resulting to compression. This suggests that a significant amount of folding in fold-thrust belts can result from an early halokinetic fold system developed during the pre-contractional passive margin evolution.

Keywords: Mesozoic halokinesis; Basement inheritance; Mixed tectonic style; Cross section balancing; South Provence margin

1. Introduction

The characteristics of the pre-contractional structures in Cenozoic orogens are fundamental to understand the factors controlling basin inversion and thrust propagation. The reactivation of preexisting crustal anisotropies and the presence of décollement levels in the sedimentary cover favor the development of a mixed thick- and thin-skinned tectonic style in fold-thrust belts (e.g., Davis and Engelder, 1985; Muñoz, 1992; Schönborn, 1992; Vergés et al., 1995; Lacombe and Mouthereau, 2002; Sherkati et al., 2006; Espurt et al., 2008; Turienzo et al., 2014; Lacombe and Bellahsen, 2016; Bestani et al., 2016). Fold-thrust belts can be superimposed on salt-bearing passive margins including preexisting halokinetic structures with sediment thickness variability (e.g., salt walls, domes, salt-cored anticlines and diapirs, and minibasins sinking into salt). Shortening in such irregular structural systems leads to the development of more complex fold-thrust belts with the influence of pre- and syn-compressional salt tectonics (e.g., Callot et al., 2007; Hudec and Jackson, 2009; Jahani et al., 2009; Peel, 2014; Kergaravat et al., 2016; Callot et al., 2016; Duffy et al., 2018). Therefore, a fundamental problem is to determine how thick-skinned, thin-skinned and salt tectonics interfere in a contractional setting and restore the geometry of the inherited structures. Cross

section balancing technique can be used to restore the pre-contractual architecture of inverted passive margins, detect the occurrence of pre-existing basement and cover structures, and estimate the magnitude of shortening.

Located in southeastern France, the Provence fold-thrust belt has experienced moderate shortening during the Campanian-Eocene N-S Pyrenean-Provence compression and was then deformed by Oligocene-Miocene Ligurian-Provence rifting events and Neogene to present-day Alpine compression (e.g., Tempier, 1987; Bergerat, 1987; Villeger and Andrieux, 1987; Hippolyte et al., 1993; Lacombe and Jolivet, 2005; Bestani et al., 2016). This fold-thrust belt superimposed on a Mesozoic passive margin that developed during the opening of the Tethys-South Provence/Pyrenean rift system (Masse and Philip, 1976; Philip et al., 1987; Lemoine and de Graciansky, 1988; Tavani et al., 2018). The Provence fold-thrust belt is also characterized by substantial upper Paleozoic basement grain, thickness variations of the Jurassic and Cretaceous sub-basins, and locally by huge volumes of middle-late Triassic evaporitic levels (Mennessier, 1959a; Caron, 1979; Ménard, 1980; Brocard and Philip, 1989; Brocard, 1991; Le Pichon et al., 2010; Guyonnet-Benaize et al., 2015; Bestani et al., 2016). These evaporitic levels, which acted as a prominent thrust décollement levels during the compressional stages, were also associated with pre-contractual salt-related structures (Mennessier, 1959a; Guieu, 1968; Angelier and Aubouin, 1976; Tempier, 1987; Philip et al., 1987; Mascle et al., 1988; Dardeau et al., 1990; Roure and Colletta, 1996; Huyghe et al., 1999; Bestani et al., 2015, 2016). Isolated diapiric salt structures were described in detail decades ago along the inverted southern Alpine Tethys-North Provence passive margin transition as, for example, the Condorcet, Propiac, Suzette, Lazer and Barles diapirs (Emré and Truc, 1978; Casagrande et al., 1989; Dardeau et al., 1990; Dardeau and de Graciansky, 1990; Huyghe et al., 1999; Graham et al., 2012). In the South Provence domain, field data, seismic reflection profiles and regional balanced cross sections revealed that middle-late

Triassic evaporites impacted the folding and sedimentation during compressional and extensional stages (Angelier, 1971; Philip et al., 1987; Roure et al., 1992; Benedicto et al., 1996; Rangin et al., 2010; Le Pichon et al., 2010; Bestani et al., 2015, 2016). The eastern Provence fold-thrust belt located between the Middle Durance/Aix-en-Provence fault zone and the Paleozoic Maures and Tanneron-Estérel massifs, displays a large NE-trending zone of outcropping middle-upper Triassic evaporites-carbonate surrounding numerous synclines of Jurassic-Cretaceous rocks (Fig. 1; Tempier, 1987; Jannin, 2011). Although some studies undeniably showed that exhumation of the Triassic rocks occurred during the Oligocene rifting along NE-trending basement fault systems (Cornet, 1970; Angelier and Aubouin, 1976; Bestani et al., 2015), numerous unconformities between Triassic evaporites and Jurassic to upper Cretaceous sequences, may suggest that halokinesis already started in the Mesozoic times (Philip, 1967; Mennessier, 1975; Philip et al., 1987; Jannin, 2011; Bestani et al., 2015; Philip, 2018a). Although the Provence basin suffered polyphase deformations during late Cretaceous and Cenozoic times, the initial structural framework of the precursor margin can be easily reconstructed using geological data and the powerful cross section balancing technique. The reconstruction of the margin will allow us to evaluate the evolution of a fold-thrust belt and foreland basin superimposed on a heterogeneous and complex evaporite-rich passive margin. The structures of the eastern Provence fold-thrust are shown in cross sections by de Lapparent (1938b), Mennessier (1959), Bathiard and Lambert (1968), Tempier (1987), Jannin (2011) and Bestani et al. (2015, 2016). These cross sections show a mixed tectonic style (thick-skinned, thin-skinned and salt tectonic styles) and a shortening magnitude ranging between ~30 and 40 km in the study area (Tempier, 1987; Bestani et al., 2015).

In this paper, we present and discuss a new interpretation of the Provence Chain in terms of an evolution of a Mesozoic halokinetic salt province and basement inheritances that are later reactivated as compressional system during the Pyrenean and Alpine orogenies. New

fieldwork results, exploration well data and previously published geological maps have been used to interpret a new regional balanced and restored cross section across the eastern Provence fold-thrust belt (Fig. 1). We analyze the geometry of the structures and timing of their deformations and derive amount of orogenic contraction. The restoration of the Mesozoic paleomargin framework of this part of Tethyan-South Provence margin provides insight into the role of an early halokinetic fold system later incorporated into a mountain.

2. Geologic framework

2.1. The eastern Provence fold-thrust belt

The Provence basin developed between the Alps to the northeast, the Central massif to the west, and the Mediterranean Sea to the south. The eastern Provence fold-thrust belt belonging east of the Rians, Arc and Beausset basins and west of the Permian depressions and Variscan Maures and Tanneron-Estérel massifs (Figs. 1 and 2) was formed above a thick middle-upper Triassic evaporitic-carbonate layer and complex array of inherited basement structures, explaining its irregular of thrust traces in map view (Bathiard and Lambert, 1968; Baudemont, 1985; Tempier, 1987). This hybrid fold-thrust belt mainly results from the ~N trending Campanian-Eocene Pyrenean-Provence compression (Bergerat, 1987; Lacombe and Jolivet, 2005; Bestani et al., 2016). This framework was then deformed by Oligocene extensional faults during the Ligurian-Provence rifting, and by Africa-Europe plate kinematics and the southern propagation of the Castellane compressional arc (Figs. 1 and 2) during Miocene to present-day (Bergerat, 1987; Villeger and Andrieux, 1987; Hippolyte et al., 1993).

2.2. Description of the stratigraphic succession and geological evolution

The regional nomenclature, lithology, age and tectonic setting of the stratigraphic succession are summarized in Fig. 3, and briefly described hereafter. We particularly defined the stratigraphy of the middle-upper Triassic rocks associated with evaporitic sequences (Figs. 4 and 5).

2.2.1. Basement: Variscan and upper sedimentary Paleozoic succession, and lower-middle Triassic red beds

The basement of the Provence domain is formed by the Paleozoic rocks unconformably overlain by lower-middle Triassic fluvial sediments. Variscan basement and overlying upper Paleozoic sedimentary succession are exposed along the southern and southeastern borders of the study area in the Tanneron-Estérel, Maures, and Cap Sicié massifs, and locally revealed by deep exploration wells (Carcès-1, Carpiagne-1, Jouques-1 and Gréoux-1 wells; Fig. 1) under the Mesozoic-Cenozoic sedimentary cover. Variscan rocks are composed of upper Carboniferous granitoids and foliated metamorphic including phyllades, micaschistes and gneisses. They are unconformably overlain by unmetamorphosed upper Carboniferous to Permian volcanoclastic and detrital successions accumulated in transtensional depocenters during the rifting of Pangea (Baudemont, 1985; Delfaud et al., 1989; Toutin-Mourin et al., 1993; Crévola and Pupin, 1994; Onézime et al., 1999; Rolland et al., 2009; Fig. 3). Surface, well and geophysical data suggest a heterogenous distribution of the upper Paleozoic depocenters associated with NNE- to SE-trending steeply-dipping normal and strike-slip faults (Bathiard and Lambert, 1968; Delfaud et al., 1989). In the western side of the Maures massif, thickness of the upper Carboniferous-Permian strata reaches more than 1200 m (Bathiard and Lambert, 1968; Cassini et al., 2003). In the Carcès-1 well, these strata reach a minimum thickness of 670 m. No upper Paleozoic sedimentary rock is found in the Jouques-1 and Gréoux-1 wells (Fig. 1). In the study area the lower-middle Triassic (middle Olenekian-Anisian) fluvial strata (Units A-B; Buntsandstein local stage; Fig. 4) consist of conglomerates, sandstones, arkoses and lutites with a mean thickness of ~40-50 m (Brocard and Philip, 1989; Toutin-Morin et al., 1994; Durand and Gand, 2007).

2.2.2. Middle-upper Triassic evaporitic-shallow marine carbonate succession

The opening of the Tethys ocean started with the deposition of evaporitic-shallow marine carbonate sedimentary systems during middle-upper Triassic times (Muschelkalk and Keuper local stages) well developed in the Brignoles-Draguignan area (Mennessier, 1959a; Caron, 1979; Figs. 1 and 2), and whose the stratigraphy was revised and divided in three evaporitic-carbonate systems (Brocard and Philip, 1989; Brocard, 1991; Toutin-Morin et al., 1993, 1994; Fig. 4). The lower system resting on the Buntsandstein sandstones consists of about 30 m-thick of alternations of dolomites, stromatolitic marls, brecciated cargneules, beds of gypsum and anhydrite (Unit C; Anhydritgruppe; basal Muschelkalk) overlain by 40 m-thick of laminated and bioturbated grey massive limestones (Unit D; lower Muschelkalk). The middle system consists of 30 m-thick of green clays and cargneules, shales, dolomitic breccias (Unit E; middle Muschelkalk) overlain by 45 m-thick of marls and thickening upward bioclastic and bioturbated grey limestones bearing a benthic fauna with crinoids, brachiopods and bivalves (Unit F; upper Muschelkalk). The upper system consists of a few tens to a hundred meters thick of white dolostones (Lettenkohle), red, ochre or yellow gypsum marls, anhydrite and shales with interbeds of dolomites (Keuper). Halite has been reported in basal Muschelkalk from salt springs of the northern Provence region (Mennessier and Modret, 1966; Mennessier et al., 1969) and in Keuper of the Jouques-1 well (Fig. 1). Rhaetian rocks consist of 30 m-thick of alternations of coquina limestones and yellow marls. Middle-upper Triassic successions also contain ankaratrite intrusions and volcanoclastic levels (Caron, 1970).

Because of salt dissolution, evaporites are poorly observed to the surface and form cargneules (Fig. 4b). Regional variations of the thickness of the middle-upper Triassic rocks are observed on the field. According to Mennessier (1959a) the thickness of the Anhydritgruppe could reach about 100 m in the Brignoles-Draguignan area (Fig. 1). Thickness of the Keuper strata oscillates between 40 m or less in the vicinity of the Maures Massif to 100 m or more in the Flayosc-Brignoles area (Fig. 1). Three exploration wells

(Carcès-1, Garéoult and Jouques-1) in the study area show major thickness increase of the middle-late Triassic strata at depth (Fig. 5). The Carcès-1 well shows 1130 m-thick of alternations of anhydrite, gypsum, dolomite and limestone beds displaying heterogenous dipplings of different values (Baudemont, 1985). The Garéoult well has cut 450 m-thick of three superimposed upper Muschelkalk-Keuper strata, displaying strong dips in the upper Muschelkalk limestones (Duvochel et al., 1977). The Jouques-1 well shows ~450 m of Keuper above thin Muschelkalk limestones. In these three wells the great increase of the thickness of the middle-upper Triassic rocks in comparison with field observations could be controlled by tectonic duplication of evaporitic units, either of the Anhydritgruppe (Carcès-1 well), or of the Keuper (Garéoult well) during the compressive stages (Bathiard and Lambert, 1968). However, the thickness variations of the evaporites could also be due to local depocenters or to lateral movement of the evaporites out from under the subsiding regions before compression. According to Toutin-Morin et al. (1993, 1994), these regional thickness variations could in part be due to a Carnian extension affecting the Triassic basement and creating coeval basement horsts and grabens.

To summarize, the middle-upper Triassic comprises three ductile marly-evaporitic levels (basal Muschelkalk, middle Muschelkalk and Keuper) considered as potential decollement levels of the sedimentary cover above the Paleozoic-Triassic (buntsandstein) basement, and probably associated with halokinesis during the Mesozoic and Cenozoic sedimentary history of the Provence region.

2.2.3. Liassic to lower Santonian succession

During Liassic to middle Jurassic period of the Tethyan rifting, the South Provence margin developed with dominantly marine carbonate sediments and major thickness variations on the field (Lemoine and de Graciansky, 1988; Léonide, 2007; Léonide et al., 2007). Liassic rocks (70 to 220 m-thick) consist of dolomites, limestones and marls (Léonide, 2007; Léonide et al.,

2007). Middle Jurassic rocks (~100 to more than 400 m-thick) consist of ammonites bearing, marly limestones, limestones and breccias deposited in a deep marine environment. Upper Jurassic strata correspond to shallow limestones and dolomites (50 to 700 m-thick). The subsidence continued during early Cretaceous associated with the opening of the Pyrenean rift system/South Provence basin between Eurasia and Sardinia-Corsica block (de Graciansky and Lemoine, 1988; Schettino and Turco, 2011; Bestani et al., 2016; Tavani et al., 2018) leading to the deposition of 500 to 800 m-thick carbonate succession on the South Provence margin, including the rudist bearing Urgonian facies (de Graciansky and Lemoine, 1988; Hibschi et al., 1992; Masse et al., 2009; Léonide et al., 2012; Masse and Fenerci-Masse, 2013). During uppermost Barremian-lowermost Aptian, the South Provence basin opened and during Aptian time, ammonites bearing limestones and marls up to 250 m-thick deposited. During upper Aptian-Albian, the basin was filled by turbiditic and basinal sediments, which include olistoliths and breccias in the southern limb of the Beausset syncline (Philip et al., 1987; Machhour et al., 1994). From uppermost Albian to lowermost Cenomanian at least, and till Santonian in some places, the Durance High uplift is associated with major erosion, weathering and bauxite development, north of the Beausset syncline (Masse and Philip, 1976; Laville, 1981; Fig. 3). The bauxite is covered by upper Cenomanian to Santonian transgressive marine carbonate to terrigenous siliciclastic sediments that reach a maximum thickness of ~1100 m in the southern limb of the Beausset syncline (Mont-Caumes area in Fig. 2; Philip, 1970; Floquet et al., 2005, 2006). Siliciclastic sediments were mainly sourced by a southward emerged basement high between Provence and the Sardinia-Corsica block (Hennuy, 2003).

2.2.4. Uppermost Santonian to Eocene Provence foreland succession

Foreland deposition and transition from marine to continental environment occurred during uppermost Santonian (Fabre-Taxy and Philip 1964; Philip, 1970; Westphal and Durand,

1990). This environment depositional change is interpreted as the onset of collision between Eurasia and Corsica-Sardinia block and the northward propagation of the Provence fold-thrust belt. Upper Cretaceous foreland sequences consist of uppermost Santonian-lower Campanian lacustrine and palustrine black limestones including lignite beds (Valdonnian and Fuvelian local stages) and middle Campanian-Maastrichtian fluvial deposits including dinosaur eggshells and bones (Begudian and Rognacian local stages). Paleocene-Eocene foreland sequences correspond to Danian red silty marls and limestones, Selandian-lowermost Ypresian marls, and Ypresian fluvial bluish micaceous sand (Sables bleutés Fm) including lacustrine Bithynia bearing limestones (de Lapparent, 1938a,b; Durand and Tempier, 1962; Angelier, 1971; Philip et al., 2017). Locally, foreland sequences include remarkable syn-tectonic conglomerates (Fig. 3) organized in alluvial fan systems with clasts derived from Mesozoic strata and Paleozoic basement (i.e., Begudian-Rognacian breccias, Danian Microcodium breccias and Touars conglomerates; Guieu, 1968; Leleu et al., 2005; Espurt et al., 2012; Philip, 2018b).

2.2.5. Oligocene rift strata

The Oligocene strata overlie unconformably a heterogeneous substratum inherited from the Pyrenean-Provence compression. These strata were deposited in N- to NE-trending grabens and half-grabens during the opening of the West European rift, then the back-arc rifting of the Ligurian basin between Provence and Sardinia-Corsica block (Hippolyte et al., 1993; Cherchi et al., 2008). In the study area, the Oligocene strata were characterized by the predominance of fluvial conglomerates (Bourdas Fm) associated to shales and lacustrine limestones deposited in local and narrow half-grabens (Angelier, 1971; Popoff, 1973; Nury, 1990; Philip et al., 2017; Fig. 3). Oligocene strata do not exceed 100 m in thickness.

2.2.6. Middle Miocene-Pliocene Alpine foreland to present-day succession

Middle Miocene-Pliocene sediments deposited during the Alpine orogeny. Langhian-Tortonian continental strata up to 50 m-thick correspond to conglomerates, sands, red to yellow marls and lacustrine limestones (de Lapparent, 1938b; Mennessier, 1959; Cornet, 1965; Fig. 3). Like Oligocene strata, the middle Miocene strata overlies unconformably a heterogeneous substratum, Triassic to Eocene in age. Following the Messinian desiccation, Pliocene continental conglomerates filled deep incised canyons and the Valensole basin, north of the study area (Clauzon et al., 1996). The present-day morphology of the Provence domain mostly results from the Messinian paleogeography (Clauzon, 1984). Pleistocene to present-day sediments correspond to torrential and periglacial alluvial deposits, and modern alluvium deposits filling the incised valleys.

3. Method

To study the structural architecture of the eastern Provence thrust belt, surface structural and sedimentological data, regional structural geometry descriptions, and well data were integrated to construct a new ~80 km-long balanced cross section across the eastern Provence fold-thrust belt extending from the Mediterranean Sea to the south and the Verdon region to the north (Figs. 1 and 2). This NNE-trending cross section is approximately parallel to the Pyrenean-Provence and Alpine tectonic transport directions (Bergerat, 1987; Lacombe et al., 1992; Hippolyte et al., 1993; Espurt et al., 2012) and no strike-slip faults have been crossed. Surface data were obtained from extensive fieldworks and from 1:50 000 Bureau de Recherches Géologiques et Minières geological maps.

Cross section balancing follows thrust tectonic concepts (Dahlstrom, 1969; Boyer and Elliot, 1982; Elliott, 1983; Shaw et al., 2005). Cross section balancing and restoration were performed using Move structural modeling software based on bed length and thickness conservation and the built-in flexural-slip algorithm. The middle-upper Triassic evaporitic-carbonate layer was not balanced during restoration because this layer is considered free to

move in three dimensions and to be eroded in successive stages of exposed diapirism. As possible, we attempt to restore the top of the carbonate Triassic strata (Muschelkalk-Keuper interface). The interpreted cross sectional architecture and restoration of the eastern Provence fold-thrust belt is shown in Fig. 6 and take into account the structural data described in sections 4 and 5. The proposed balanced cross section is one possible construction in depth because of the lack of seismic reflection data in the study area but the most realistic solution consistent with the available surface and subsurface geological data. For more details and clarity of this long cross section, it has been cut and presented in three sub-sections in Figs. 7, 8 and 9. Details of the geological map are also shown in Fig. 10. The cross section was restored for a lower Campanian state (Fig. 6b), i.e., before foreland thrust propagation as recorded by first middle Campanian syn-tectonic deposits in Provence (Guieu, 1968; Leleu et al., 2005; Espurt et al., 2012; Philip, 2018b Fig. 3).

4. Description of the thrust systems and timing of shortening

The following structural description of the thrust systems is divided into three parts regard to the geological map, stratigraphy and the balanced cross section which are presented in this study: from north to south, the northern Provence units, the southern Provence units, and the coastal inner units (Figs. 2, 3 and 6).

4.1. The northern Provence units

The northern Provence units are composed of the Moissac anticline, the north-verging Fox-Amphoux/Sillans and Pontevès thrust systems, and the south-verging Bras imbricate (Figs. 7 and 8). North and south of the Moissac anticline, upper Jurassic strata are flat and unconformably covered by continental Miocene-Pliocene strata. The Moissac anticline is mantled by upper Jurassic strata exhibiting a 40° north-dipping northern limb and a 12° south-dipping southern limb. Eastward, a south-verging thrust transported upper Triassic and Jurassic rocks of the Moissac anticline upon upper Cretaceous-Ypresian strata of the Aups

syncline. South of a large 3° south-dipping homocline of upper Jurassic strata, upper Cretaceous to Eocene strata are involved in the Amphoux syncline. The vertical southern limb of the Amphoux syncline is overthrust by middle Jurassic strata of the Fox-Amphoux thrust system (Fig. 7c). Along cross section, the structural frame of the Fox-Amphoux thrust system corresponds to two major north-verging imbricate thrust sheets (Fox-Amphoux and Sillans) transporting the Rognette syncline filled by upper Cretaceous to Eocene strata. The frontal Fox-Amphoux thrust dips ~17° to the south (Fig. 7c), becoming flat to the north as indicated by klippe of upper Jurassic limestones above Eocene strata of the Amphoux syncline (Fig. 2). Westward, these east-trending thrusts connect with the NNE-trending Quinson thrust (Fig. 2). Southward, the north-dipping to overturned upper Cretaceous to Ypresian strata of the southern limb of the Rognette syncline are overthrust by the north-verging Pontevès thrust system (Fig. 7d). This thrust system, linked with at least two branches, transported the prominent perched synclines of the Bessillon massif and the large Correns syncline with relatively lower structural reliefs, both armed of middle-upper Jurassic limestones (Tempier, 1972). The Bessillon and Correns synclines are separated by an east-trending narrow Triassic ridge connected westward with the Barjols Triassic depression (Fig. 10a).

Southward, the Bras imbricate corresponds to three south-verging thrusts (Miraval, Vins and Brignoles) separated by synclines (Fig. 10a). The detailed geometry of the Bras imbricate is shown in Fig. 8a. The structure of the Bras imbricate has been described by Mennessier (1975) and Godet (1976) using numerous surface cross sections of excellent quality. The deep geometry of the structure benefited from the subsurface data of the Carcès-1 exploration well located 6 km to the east (Fig. 10a). The Correns syncline is limited to the south by the ENE-trending Miraval anticline cored by Triassic evaporites, connecting the large Triassic depressions of Barjols and Carcès (Fig. 10a). The Carcès-1 well data located on the Miraval anticline reached the Permian/Carboniferous basement under ~1.1 km-thick of middle-upper

Triassic strata (Fig. 5). The Permian strata crop out immediately southward in the Terrubi anticline underlined by lower Triassic red beds (Figs. 4d and 10a). The Vins thrust transported to the south smaller and asymmetric synclines of Jurassic rocks above continental middle Campanian strata (Begudian) of the Val syncline. Southward, the Brignoles thrust transported a broad antiform of internally folded Triassic and lower-middle Jurassic strata above 20° north-dipping Jurassic strata of the northern limb of the Mazaugues-Engardin anticline (Figs. 8a and 10a).

4.2. The southern Provence units

The Loubé thrust corresponds to the eastern continuation of the Sainte-Baume thrust (Mennessier, 1959b; Thiele, 1972; Eisenlohr, 1974a,b; Aubouin et al., 1976; Fig. 2). Westward, the Sainte-Baume thrust transported northward the Beausset syncline (Bestani et al., 2015; Fig. 1). Eastward, the geometry of the Loubé thrust is relatively more complex including salt-cored anticline with internal disharmonic folding (e.g., Garéoult and Méounes) and syncline structures (Rocbaron, Saint Clément massif, Valcros, eastern Beausset), and north-trending fault zones injected of Triassic evaporites (Cornet, 1957; Bathiard and Lambert, 1968; Eisenlohr, 1974a,b; Duvochel et al., 1977; Figs. 9 and 10b). To the north, the Loubé massif corresponds to a large anticline cored by Liassic strata with second-order internal folding. This anticline has a 7° north-dipping forelimb and a 10° south-dipping backlimb. The frontal part of the Loubé thrust is constituted by the Camps system where shortening is accommodated by folded Santonian-lower Campanian strata (Fig. 10a). The footwall of the Loubé thrust is constituted by 30° south-dipping Jurassic-Cretaceous strata of the southern flank of the Mazaugues-Engardin anticline, which extend below the Loubé massif (Eisenlohr, 1974a; Fig. 9a). Southward, the section crosses the Garéoult anticline cored by middle-upper Triassic strata. The N-S structure of the Garéoult anticline can be explained as resulting from the duplication at depth of the middle-upper Triassic evaporitic-carbonate

strata according to subsurface data of the Garéoult well (Duvochel et al., 1977; Figs. 5 and 9a). We propose that the slip of the imbricate was passively accommodated on an inferred south-verging backthrust (Fig. 9a,c). The Saint-Clément massif is an isolated syncline formed by Rhaetian to Bathonian limestones and upper Jurassic dolomites in fold axis (Fig. 10b). It is transported on the Garéoult imbricate and overthrust by the Belgentier anticline to the south. The Belgentier anticline is cored by Triassic strata and transported northward the Valcros and eastern Beausset synclines. This anticline is interpreted as overlying a basement horst of Permian rocks (exposed to the east) and bounded by steeply-dipping normal faults (Fig. 10b). Preserved normal faults are common within Triassic and Permian strata in the vicinity of the Cuers town (Figs. 9d and 10b) and north of the Maures Massifs (Fig. 1). These faults differ from E-trending steeply-dipping normal faults probably Oligocene or younger in age and cutting through the entire sedimentary pile (Eisenlohr, 1974a,b).

4.3 The coastal inner units

The coastal inner units are composed of the Toulon and Bandol units in the front of the Cap Sicié basement imbricate (Tempier, 1987; Bestani et al., 2015; Fig. 10c). The Toulon and Bandol units form a relay system of two north-verging cover thrust systems overthrusting middle-upper Cretaceous strata of the Beausset syncline. Our cross section cuts the eastern edge of Toulon unit (Figs. 2 and 9a) detached in the Triassic evaporites and carbonates (Haug, 1925; Gouvernet, 1963; Philip et al., 1987). Jurassic sedimentary sequences of the Toulon unit are relatively thinner (~500 m) than those of the Beausset syncline to the north (>1300 m; Gouvernet, 1963; Cornet, 1967; Tempier, 1972; Léonide, 2007). The Toulon unit is composed of the northern Brémone thrust (associated with the Coudon thrust in the footwall of the Brémone thrust to the east) and the southern Faron thrust system (Gouvernet, 1963; Figs. 9a and 10c). The thrust systems are cut by numerous normal faults probably Oligocene or younger in age. The Bandol thrust sheet is formed by thick (>1000 m) Jurassic strata detached

above upper Triassic evaporites (Fig. 10c). This thrust sheet is removed by erosion east of the Cap Sicié massif (Figs. 2 and 9a). Santonian-lower Campanian strata of the Beausset syncline are tectonically overlain by middle-upper Triassic and Liassic rocks (e.g., Pibarnon and Beausset Triassic coverings; Fig. 10c), related to the Bandol thrust sheet (Bertrand, 1887; Haug, 1925; Gouvernet, 1963). These Triassic coverings indicate a minimum northward displacement of 5 km for the Bandol thrust sheet with respect to its footwall (i.e., the southern flank of the Beausset syncline; Tempier, 1987). Westward, the footwall of the Bandol thrust sheet is constituted by the Saint-Cyr Triassic doming (Fig. 10c and 11) where lower Santonian limestones and conglomerates unconformably overlie middle Triassic Muschelkalk limestones (Philip, 1967; Philip et al., 1987; Bestani et al., 2015).

The Cap Sicié imbricate defines the southern edge of the study area along the Mediterranean coast (Figs. 2 and 9a). It is made of Variscan metamorphic rocks, upper Carboniferous to Permian volcanoclastic continental strata and lower-middle Triassic strata. The tectonic window of Saint-Mandrier anticline (Zürcher, 1893) shows Permian and lower-middle Triassic strata tectonically covered by Variscan schists and quartzites of the north-verging Cap Sicié thrust (Haug, 1925; Tempier, 1987).

4.4. Record of contractional deformations

The contractional deformation in the Provence fold-thrust belt would be first recorded by the marine to continental environment change in the uppermost Santonian strata in the southern Provence units (Fig. 3). This earliest contraction might record to the propagation of inner units (e.g., the Toulon and Bandol units). Northward, thrust activity of the Sainte-Baume/Loube thrust system was recorded by Maastrichtian (Rognacian) breccias (Guieu, 1968; Bestani et al., 2015). In the northern Provence units, the activity of the Pontevès and Fox-Amphoux thrust systems has been recorded later by Danian Microcodium breccia deposits in the Rognette and Amphoux synclines (Angelier, 1971, 1974; Touraine, 1978;

Philip et al., 2017; Fig. 12a). This chronology of thrust propagation, which is deduced from synorogenic deposits in different places and times, suggests a classical hinterland to foreland sequence of thrusting.

Pyrenean-Provence folds and thrusts of the study area are occasionally cut by steeply-dipping normal faults and doming of Triassic evaporites along NNE- to NW-trending fault zones associated with Oligocene syn-tectonic conglomerates (Angelier, 1971; Angelier and Aubouin, 1976; Bestani et al., 2015). Evidence of post-Oligocene deformations are clearly recognizable in several places of the Triassic depression of Barjols (near Varages, Bras and Rougiers towns in Fig. 2). In these places, Oligocene or Miocene strata are folded, overturned and affected by thrust faults (Figs. 12b,c). This suggests that a significant Alpine shortening occurred in the study area (Bergerat, 1987; Villegier and Andrieux, 1987; Hippolyte et al., 1993). The Alpine shortening is still active in the northern part of the eastern Provence fold-thrust belt as revealed by present-day seismic events ($M_w < 3.5$) distributed in the sedimentary cover and basement (Cushing et al., 2008; *BCSF catalog*, <http://renass.unistra.fr>).

5. Pre-contractinal halokinetic features in the South Provence margin

Many fold-thrust belts around the world such as the Zagros (Jahani et al., 2009; Callot et al., 2012), the Atlas (Saura et al., 2014; Gharbi et al., 2015; Teixell et al., 2017) or the southern Pyrenees (López-Mir et al., 2014; Saura et al., 2016) are characterized by pre-contractinal halokinetic structures including salt-cored anticlines, domes, diapirs or walls together with minibasins (Trusheim, 1960; Worrall and Snelson, 1989). Classically, the ductile salt is evacuated from under the subsiding minibasins by sedimentary loading and expelled laterally and toward the surface in diapiric structures (e.g., Peel, 2014; Callot et al., 2016). Timing of halokinetic processes is recorded by the syn-salt tectonic infilling of the minibasins and by intraformational unconformities (growth wedges) in the minibasin flanks. Analysis of the geological mapping, field data and the new balanced cross section and the

integration of previous studies provide evidence for Jurassic-lower Santonian pre-contractional halokinetic signatures in the eastern Provence fold-thrust belt.

The zoomed geological maps of Fig. 10 illustrate a polygonal array of salt-cored anticlines that enclose synclines of Rhaetian-Jurassic calcareous rocks in northern and southern Provence units. Middle-upper Triassic evaporitic-carbonate strata of the anticline cores are often unconformably overlain by various Mesozoic rocks ranging from Rhaetian to upper Jurassic. In the northern Provence unit (Fig. 10a), the geological mapping and surface cross sections of Mennessier (1975) show major thickness variations and growth wedges in the Rhaetian-Jurassic infilling of the Val syncline that we interpret as a minibasin structure. The minibasin shape of the Val syncline is clearly defined by the three-dimensional view of Fig. 13. The palinspastic reconstruction of Fig. 8b demonstrates that the Bras imbricate involved several Rhaetian-Jurassic calcareous synclines with characteristic minibasin geometries, separated by domes of Triassic evaporites. Minibasins are associated with minor NNW- to NE-trending syn-sedimentary normal faulting together with breccia deposits and slumping as observed in Bathonian-Bajocian carbonate strata of the Correns syncline (Fig. 8c). In the Brignoles thrust, a narrow syncline of middle Jurassic breccias of lower-middle Jurassic calcareous clasts in an evaporitic-carbonate matrix lie unconformably above upper Triassic evaporites (Figs. 8d and 10a; Eisenlohr, 1974a). These sedimentary breccias can be interpreted as a residual cap-rock above the Brignoles Triassic dome that was partly exhumed during the middle Jurassic times in this zone. The sinking of these minibasins into Triassic evaporites and the growth of the salt domes would have been initiated in Rhaetian and then continued during Jurassic times.

Similar halokinetic geometries are observed in the southern Provence unit (Fig. 10b). We interpreted the Garéoult anticline as an inherited salt dome which has been uplifted during the Jurassic times (Fig. 9b). This is consistent with decreasing thicknesses of the Bathonian-

Bajocian strata of the Loube and Saint-Clément massifs toward the Garéoult Triassic dome (Cornet, 1967; Eisenlohr, 1974a). Like the Brignoles Triassic dome, the northern flank of the Garéoult dome shows similar folded syn-sedimentary middle-upper Jurassic breccias overlying upper-middle Triassic strata previously mapped by Eisenlohr (1974a) (Figs 9e,f). The surface data and the palinspatic restoration suggest that the Saint-Clément massif and the eastern Beausset synclines are preserved minibasins enclosed by the salt domes of Garéoult and Belgentier (Fig. 9; Jannin, 2011).

Previous studies across the Beausset syncline (Philip, 1967, 1970; Philip et al., 1987; Fig. 10c) showed major thickness and facies changes in the middle-upper Cretaceous succession that depict depocenters and structural highs (Fig. 14). The NNW-trending Clavelle trough is mainly filled by thick (~330 m) upper Aptian-Albian turbiditic and basinal succession including breccia beds of Mesozoic clasts. The Mont-Caumes depocenter shows thick (~350 m) upper Turonian-Coniacian sandstones and breccias. Northward, the east-trending Beausset depocenter (Fig. 11a) shows more than 600 m-thick of Turonian-lower Santonian siliciclastic sediments (Philip et al., 1987; Bestani et al., 2015). The sediments accumulated in these depocenters thin rapidly or onlap to the depocenter edges with minor normal faulting (Figs. 11a and 14). The western major NNW-trending Saint-Cyr high shows transgressive lower Santonian rudist limestones and conglomerates which unconformably overlie middle Triassic Muschelkalk limestones (Fig. 11b; Philip, 1967). These major thickness variations record eastward and northward migration of the depocenter from upper Aptian to lower Santonian times. The general geometry archived by these depocenters and their sequence development would have been controlled by listric normal faulting (i.e., Clavelle depocenter) or basement faulting but also by Triassic salt movement at depth (Philip et al., 1987). The sediment load in the middle-upper Cretaceous depocenters could have been accommodated by the evacuation of an inferred Triassic salt layer from under the subsiding zones toward the adjacent Saint-Cyr

Triassic doming as suggested by Philip et al. (1987). In addition, Philip et al. (1987) argued for a depositional hiatus of Jurassic (and lower-middle Cretaceous) succession above the Saint-Cyr Triassic doming, whereas a continuous and thick Jurassic succession is found to the east (Fig. 10c). This suggests that halokinetic activity may have started during the Jurassic times like in the northern regions.

6. Cross section balancing, basement structures and shortening

The combination of new surface structural data together with well data and previously constructed cross sections (Mennessier, 1959a, Bathiard and Lambert, 1968; Tempier, 1987) allowed us to build a geodynamic model of the deep structural architecture of the eastern Provence fold-thrust belt (Fig. 6).

As observed in the Maures massif, the horizontal stress induced by the Pyrenean-Provence and Alpine contractional episodes seems to have not reactivated high-angle upper Paleozoic basement normal faults as reverse faults. Field data rather suggest that the low-angle basement thrusts superimposed on Variscan metamorphic foliation (or inherited shear zones) and the upper Carboniferous-Permian normal fault systems were transported passively above short-cut thrusts (Figs. 15) as described in previous works (Bathiard and Lambert, 1968; Baudemont, 1985; Tempier, 1987). For instance, this foliation-parallel slip has been previously proposed for basement thrusting in the Sierras Pampeanas of Argentina by Bellahsen et al. (2016).

We modeled that the deep structure of the eastern Provence fold-thrust belt is composed of deep basement thrusts as observed in the Cap Sicié and the Maures massifs (Figs. 2 and 15a). The shortening of these basement thrusts was accommodated upward into thin-skinned thrusts detached in ductile middle-upper Triassic rocks (Bathiard and Lambert, 1968) and by the inversion of the Mesozoic halokinetic structures. Cross section balancing suggests that the shortening of the cover thrusts was fed by three north-verging basement thrusts under the

southern Provence and Toulon-Bandol units, and a single south-verging basement thrust under the northern Provence units (Fig. 6). The balanced cross section suggests that the shortening of the southern basement thrust system is distributed in the following way in the cover: the shortening of the upper Cap Sicié basement thrust is accommodated in the Bandol and Toulon units; the one of the intermediate basement thrust in the Belgentier thrust, Garéoult imbricate and Loube thrust; the one of the lower thrust in the Mazaugues-Engardin syncline, Brignoles thrust, Vins syncline and Vins thrust. Our structural interpretation of the Loube thrust does not totally differs from model of Eisenlohr (1974a). We propose that the Jurassic cover of the Loube massif was globally coupled with the Triassic strata of the Garéoult imbricate and modeled that this imbricate was entirely transported onto the Loube thrust (as well as the Saint-Clément massif) over the Mazaugues-Engardin syncline with a minimum slip of 3.6 km (Fig. 6). Contrary to Eisenlohr (1974a), we propose a progressive eastward decrease of the displacement of the Sainte-Baume/Loube thrust which is consistent with geological mapping and eastward disappearance of the frontal thrust trace (Bathiard and Lambert, 1968; Aubouin et al., 1976; Fig. 1). The south-verging behavior of the northern basement thrust has been also suggested to interpret the deep structure and structural culmination of the Sainte-Victoire System to the west (Espurt et al., 2012; Fig. 1). We modeled that the shortening of this basement thrust was accommodated here by a 30° north-dipping short-cut thrust through a southern paleo-horst. This short-cut thrust transported southward Permian and lower-middle Triassic detritic strata (Terrubi anticline in Fig. 10a) and fed the slip of the Vins thrust system. This geometrical interpretation is consistent with a north-dipping basement normal fault between the Miraval salt-cored anticline and the Vins thrust system. This inherited normal fault would be responsible for the major northward thickening increase of the middle-upper Triassic rocks in comparison to the southern horst (Fig. 6).

The Provence fold-thrust belt recorded the cumulated horizontal shortening of the Pyrenean-Provence and Alpine contractional episodes (Bestani et al., 2016). The comparison between the balanced and restored cross sections and the integration of pre-contractional halokinetic structures shows a shortening value of 28.5 km or 24.8% (Fig. 6). This value is a minimum due to the underestimated internal shortening of the ductile evaporitic intervals and the uncertainty concerning the thrust displacement where hanging wall cut-offs are eroded (e.g., Bandol thrust sheet). This shortening value is smaller than the 30 and 40 km of shortening amounts calculated along lateral sections by Tempier (1987) and Bestani et al. (2015), respectively. Although the structure of the thrust belt mainly results from the Pyrenean-Provence compression (Bestani et al., 2016), folded Oligocene and middle Miocene strata in the study area undeniably suggest major reactivation of the structures during the Alpine compression (Figs. 12b,c). Nevertheless, we are unable at this stage to quantify the Alpine shortening amount along our cross section because Oligocene and Miocene strata are poorly preserved in the study area (Fig. 2).

In our structural model, we calculated that the southern north-verging basement thrusts accommodated 20.2 km of shortening, while the northern south-verging basement thrust accommodated only 1.6 km of shortening. The resting shortening amount, i.e., 6.7 km, was accommodated by thin-skinned structures of Miraval, Pontevès, Fox-Amphoux, and Moissac. We propose that these structures accommodated the general northward underthrusting of the Provence basement at depth (Fig. 6). This emplacement is recorded at least by Danian syn-tectonic breccias at the front of the Fox-Amphoux and Pontevès thrusts (Figs. 2 and 12a).

7. Discussion

7.1. Origin of the pre-contractional halokinetic features

Differential sedimentary loading, erosion, extension and initial thickness variations of the salt layers can initiate halokinetic movements (e.g., Nalpas and Brun, 1993; Jackson and

Vendeville, 1994; Peel, 2014; Harding and Huus, 2015). Basement extension can also influence the growth of salt structures (e.g., Jackson and Vendeville, 1994; Coward and Stewart, 1995; Warsitzka et al., 2015). Inherited upper Carboniferous-Permian high-angle normal fault systems are well described in the Maures and Tanneron-Estérel massifs (Baudemont, 1985; Delfaud et al., 1989; Toutin-Morin and Bonijoly, 1992; Toutin-Morin et al., 1992), and inferred under the sedimentary cover of the Provence fold-thrust belt (de Lapparent, 1938b; Tempier, 1987; Roure and Colletta, 1996; Espurt et al., 2012). Field data and cross section construction suggest that the upper Paleozoic extensional framework is greatly preserved and only passively transported above basement thrusts (Figs. 6 and 15). A Triassic reactivation of basement normal faults was described by Toutin-Morin et al. (1992). However, we have no evidence for basement faulting during Jurassic and Cretaceous times excepted in the inner zones (Bandol and Toulon units, Philip et al., 1987; Nerthe unit, Tempier, 1987) or along NNE-trending Middle Durance/Aix-en-Provence fault zone (Roure et al., 1992; Fig. 1). In these zones local halokinetic structures overlie major steeply-dipping basement faults controlling thickness variations of the Mesozoic rocks (Tempier, 1987; Bestani et al., 2016). Rhaetian-Jurassic halokinetic movements in eastern Provence are mostly related to the middle-upper Triassic evaporitic-carbonate strata. We propose that the initiation of salt movements was controlled by the initial geometry of the Triassic evaporitic-carbonate strata and extensional basement faulting (Jackson and Vendeville, 1994; Warsitzka et al., 2015). Thickness variations of the middle-upper Triassic evaporitic-carbonate strata might have been controlled by tectonic deformations and disharmonic folding of the ductile evaporitic-carbonate units during the Pyrenean-Provence and Alpine compressions (e.g., Mennessier, 1959a; Bathiard and Lambert, 1968; Duvochel, 1977) as observed in the Garéoult and Méounes structures (Figs. 6 and 10b). However, the basement faulting during the Triassic rifting might rather explain the significant thickness variations of the middle-upper Triassic

evaporitic-carbonate strata above horst and graben systems along the cross section. We propose that salt movement was mainly controlled by the initial geometry of the middle-upper Triassic evaporitic layers then driven by the Mesozoic sedimentary loading effect of the neighboring minibasin depocenters together with minor basement extension during Tethyan-South Provence rifting.

Halokinesis are mainly recorded by growth strata and erosional truncations in the Rhaetian-Jurassic carbonate systems and locally middle-upper Cretaceous carbonate to siliciclastic systems infilling of the minibasins and unconformities above the Triassic domes. Further accurate analyses of the facies and sedimentation evolution of the halokinetic sequences are required to better illustrate the development of these salt-related carbonate systems. Meanwhile, the geometry of the halokinetic sequences is conformable with wedge halokinetic type sequence described by Giles and Rowan (2012). Most of the structures correspond to large salt-cored anticlines. Jurassic exhumation of the Triassic rocks is only suspected in the Brignoles and Garéoult domes. The lower Campanian restoration shows that the unconformity of the Durance high erosion is only slightly deformed with long-wavelength depocenters north and south of the Brignoles dome (Figs. 3 and 6). Although subsurface data and cross section construction suggest that the initial evaporite layer is thick enough to drive halokinesis ($>$ to 1 km), minibasin structures of the study area show neither major post-Jurassic halokinesis (except locally in the southern flank of the Beausset syncline during middle-upper Cretaceous extension and along deep-seated NNE-trending basement fault zones during the Oligocene extension; Fig. 2) nor pre-contractational overturned flap (Rowan et al., 2016). A flap geometry is only suspected in the northern limb of the Val syncline (Figs. 8a and 13). Along the cross section, the carbonate intervals in the middle-upper Triassic could have prevented weld contact between bottom of the minibasins and the basement. This rheological control may have influenced the evacuation of the evaporitic material and the rise

of the dome, blocking the evolution of the halokinetic structures for the establishment of major flap geometries.

The eastern Provence fold-thrust belt can be interpreted as an inverted isolated-minibasin province in the sense of Duffy et al. (2018). We have shown that the general tectonic framework of the eastern Provence fold-thrust belt incorporated numerous Rhaetian-Jurassic (and locally middle-upper Cretaceous) halokinetic structures, including domes and minibasins, which have been reactivated during the Pyrenean-Provence and Alpine compressions as observed intermittently along the inverted southern Alpine Tethys-North Provence passive margin transition (Emré, 1977; Casagrande et al., 1989; Dardeau et al., 1990; Dardeau and de Graciansky, 1990; Graham et al., 2012).

As previously suggested by Philip et al. (1987) and Bestani et al. (2016), the South Provence margin shows major similitudes with the Pyrenean Rift system, which is also characterized by diachronic pre-contractional halokinetic structures related to the upper Triassic Keuper evaporites (including salt-core anticlines, minibasins and raft tectonics) during Mesozoic times (Canérot et al., 2005; Biteau et al., 2006; Lagabrielle et al., 2010; López-Mir et al., 2014; Saura et al., 2016). Halokinetic deformations would start somewhat later in the Pyrenean domain (late Jurassic) and maybe also synchronously with small extensional basement deformation as described in the Eastern Bay of Biscay and the Basque-Cantabrian basin (Ferrer et al., 2012; Cámara, 2017).

7.2. Evolution of the halokinetic features during shortening

Field examples and analog modeling (e.g., Rowan and Vendeville, 2006; Callot et al., 2007; Jahani et al., 2009) show that during shortening, preexisting salt structures localize preferentially the deformation. Inherited domes or diapirs are often squeezed, the evaporitic material being expelled along-strike and toward the surface. The comparison between balanced and restored cross sections shows that the cover thrust systems of eastern Provence

superimposed on preexisting salt domes (Fig. 6). The thick-skinned shortening was accommodated by internal deformation and thrusting in the middle-upper Triassic rocks and by upper large cover thrusts (Bathiard and Lambert, 1968). As suggested by analog experiments in Callot et al. (2007), the cross section shows that the general shape of the domes with gentle dipping limb ($\sim 15^\circ$), controlled the propagation of the ramps toward the surface and fostered the formation of long hanging-wall flat in thin Jurassic rocks of the former domes (e.g., Fox-Amphoux thrust).

In northern Provence units, the restoration of the cross section suggests initial huge volume of the middle-upper Triassic evaporitic-carbonate strata (Fig. 6). The large difference of volume of these strata between the present-day and restored stages may result from the dissolution of the salt. We also propose that the \sim N-trending thick-and thin-skinned shortening led to lateral evacuation of ductile middle-upper Triassic rocks toward the Barjols and Carcès Triassic depressions (Fig. 2). In the Barjols depression, the Triassic evaporitic-carbonate beds show significant fold systems which are consistent with a westward salt flow direction as suggested by Baudemont (1985). Field data do not allow us to determine if the overlying upper Cretaceous basins in the northern Provence units have been affected by halokinesis (Fig. 6). Meanwhile, this lateral expulsion may have also coupled with later syn-tectonic sedimentary loading of the Maastrichtian-Eocene Rognette and Amphoux depocenters. This example of lateral expulsion of the evaporitic material is also clearly illustrated by the map geometry of the northeastern branch of the Barjols Triassic depression (Fig. 2; Angelier and Aubouin, 1976). In this zone a NW-trending band of Triassic rocks exhibits a peanut-like shape (major squeezing near Varages town) that could result from the evolution of a salt structure (Callot et al., 2007) under at least a NE-trending post-Oligocene compression (see section 4.4. and Fig. 12b).

Evaporitic intervals are commonly observed in the upper Cretaceous and Paleocene rocks of the Amfoux and Arc basins (Corroy, 1957) suggesting that diapiric piercing to the surface occurred during Pyrenean-Provence shortening. Surface exposition of the diapiric structures after the Pyrenean-Provence compression may explain why these structures have been easily reactivated during the Oligocene extension and Alpine compression (Angelier and Aubouin, 1976). In the southwestern part of the Beausset syncline, Jurassic-lower Santonian halokinetic structures have undeniably controlled the position of the north-verging Bandol thrust sheet (Philip et al., 1987). Although evaporitic intervals are not found in the Santonian-lower Campanien strata of the Beausset syncline, the Pibarnon and Beausset Triassic coverings may constitute relics of an allochthonous salt sheet (canopy) developed from the Saint-Cyr Triassic doming (Fig. 10a). The early Pyrenean-Provence shortening may have driven salt migration and the northward expulsion of the Saint-Cyr evaporites on basin floor at the front of the Bandol thrust. For instance, this compression-driven salt migration has been previously described in the fold-thrust belt of the Sivas basin by Kergaravat et al. (2016). Relationships between salt migration and early thrusting need to be precise and require further considerations in this place.

7.3. Implication for shortening calculation in inverted salt province

During inversion of an extensional salt province, thrusts propagate through into a heterogeneous and folded sedimentary pile resulting from the early halokinesis. Along our cross section, the line-length unfolding of the Rhaetian-Middle Jurassic strata suggests a halokinetic pre-contractual folding ranging between 2.6% and 6.6% (Fig. 16). This shows that the horizontal shortening magnitude calculated in inverted salt provinces can be overestimated. Thus, a significant amount of folding in the salt-type fold-thrust belts can result from early halokinetic deformations during the passive margin evolution. Hence, the higher shortening amount calculated along lateral balanced cross sections (Tempier, 1987;

Bestani et al., 2015) needs to be revised because of the pervasive of Mesozoic halokinetic features in Provence.

8. Conclusion

In this study, new surface structural data together with exploration well data and previously published geological maps have been used to build a ~80 km-long balanced and restored cross section across the eastern Provence fold-thrust belt. These have allowed us to better constrain the structural architecture, tectonic style, and kinematics of this mixed thin- and thick-skinned fold-thrust belt and provide new insight into the Mesozoic halokinetic extensional structure.

The cover thrusts involve numerous pre-contractional halokinetic structures related to the ductile middle-upper Triassic evaporitic strata. Palinspastic reconstruction and field data indicate that these structures corresponded to salt-like dome structures and salt anticlines separating minibasins. Halokinesis is mainly recorded by growth strata, normal faulting gravitational instabilities in the Rhaetian-Jurassic carbonate systems infilling of the minibasins and unconformities above the Triassic domes. Some structures in the inner zones were active until the upper Aptian-lower Santonian period. Minibasin development has been mainly driven by sediment loading. However, the initiation of salt movements might be controlled by the initial geometry of the Triassic evaporitic-carbonate layers and basement extensional faulting.

The basement thrusts superimposed on Variscan metamorphic foliation (or inherited shear zones) and propagated through inherited upper Paleozoic extensional systems with steeply-dipping faults. The basement shortening is accommodated upward in large cover thrusts detached in middle-upper Triassic strata and by structural inversion of the Mesozoic halokinetic structures.

The comparison between the balanced and restored cross sections shows a minimum shortening of 28.5 km (i.e., 24.8%) across the Provence fold-thrust belt. This value recorded

the cumulated horizontal shortening of the Pyrenean-Provence and Alpine contractional episodes between upper Cretaceous to present-day. Preexisting salt structures have controlled thrust emplacements and their kinematics. The general shape of the salt domes with gentle dipping limb ($\sim 15^\circ$), controlled the propagation of the ramps, and internal deformation and duplexing into the domes.

The eastern Provence fold-thrust belt involved preexisting halokinetic folding (salt domes and minibasins) which can be misinterpreted as resulting to compression. This study suggests that a significant amount of folding in fold-thrust belts can result from halokinetic movements during the passive margin evolution stage.

Acknowledgments

This research project was financed by the Commissariat à l'Énergie Atomique et aux Énergies Alternatives (CASHIMA program) and the French CNRS-INSU program SYSTER 2017. Midland Valley is acknowledged for providing academic license of Move for structural modeling. We acknowledge Rod Graham and two anonymous reviewers for the constructive comments which greatly helped us to improve our manuscript.

References

- Angelier, J., 1971. La partie septentrionale de la bande triasique de Barjols (Var). Thèse de 3e cycle, Paris. Première partie, 194 p.
- Angelier, J., 1974. L'évolution continentale de la Provence septentrionale au Crétacé terminal et à l'Eocène inférieur : la gouttière de Rians-Salernes. Bulletin du BRGM, (2), I, n° 2, 65-83.
- Angelier, J., Aubouin, J., 1976. Contribution à l'étude géologique des bandes triasiques provençales : de Barjols (Var) au bas Verdon. Bulletin du BRGM, (2), I, n° 3, 187-217.
- Aubouin, J., Chorowicz, J., 1967. Le chevauchement sud-Provençal: De l'Etoile à la Sainte-Baume, Bull. Soc. Geol. Fr., 7, 600–608.
- Aubouin, J., Chorowicz, J., Thiele, R., 1976. La terminaison orientale du chevauchement sud-provençal : de la Sainte-Baume à la Loube et au Candelon. Bull. Soc. Geol. Fr., 7, XVIII, n°1, 179-190.
- Bathiard, M., Lambert, C., 1968. Rapports entre la tectonique de socle et la tectonique de couverture sur la bordure ouest des Maures. Bull. Soc. Geol. Fr., 7, 428-435.

- Baudemont, D., 1985. Relations socle-couverture en Provence orientale. Evolution tectonosédimentaire permienne du bassin du Luc (Var). Thèse de l'Université Louis Pasteur. Strasbourg, 204 p.
- Bellahsen, N., Sébrier, M., Siame, L., 2016. Crustal shortening at the Sierra Pie de Palo (Sierras Pampeanas, Argentina): near-surface basement folding and thrusting. *Geol. Mag.*, 153 (5/6), 992-1012.
- Benedicto, A., Labaume, P., Séguret, M., Séranne, M., 1996. Low-angle crustal ramp and basin geometry in the Gulf of Lion passive margin: Oligocene-Aquitainian Vistrenque graben, SE France, *Tectonics*, 15, 1192–1212, <http://dx.doi.org/10.1029/96TC01097>.
- Bergerat, F., 1987. Paléo-champs de contrainte tertiaires dans la plate-forme européenne au front de l'orogène alpin, *Bull. Soc. Géol. Fr.*, 8, III, n°3, 611-620.
- Bertrand, M., 1887. Ilot triasique du Beausset (Var). Analogie avec le bassin houiller franco-belge et avec les Alpes de Glaris. *Bull. Soc. géol. Fr.*, (3), XV, 667-702.
- Bestani, L., Espurt, N., Lamarche, J., Floquet, M., Philip, J., Bellier, O., Hollender, F., 2015. Structural style and evolution of the Pyrenean-Provence thrust belt, SE France, *Bull. Soc. Géol. Fr.*, 186, 223–241.
- Bestani, L., Espurt, N., Lamarche, J., Bellier, O., Hollender, F., 2016. Reconstruction of the Provence Chain evolution, southeastern France, *Tectonics*, 35, <http://dx.doi.org/10.1002/2016TC004115>.
- Biteau, J.-J., Le Marrec, A., Le Vot, M., Masset, J.-M., 2006. The Aquitaine Basin. *Petroleum Geoscience*, 12(3), 247–273. <https://doi.org/10.1144/1354-079305-674>.
- Boyer, S. E., Elliott, D., 1982. The geometry of thrust systems, *AAPG Bull.*, 66, 1196–1230.
- Brocard, C., Philip, J., 1989. Précisions stratigraphiques sur le Trias de la Provence orientale : conséquences structurales et paléogéographiques. *Géologie de la France*, 3, 27-32.
- Brocard, C., 1991. La plate-forme provençale au Trias moyen : un modèle de rampe carbonatée en milieu restreint. Thèse de l'Université de Provence. 227 p. XIII pl.
- Callot, J.P., Jahani, S., Letouzey J., 2007. The role of pre-existing diapirs in fold and thrust belt development. In: Lacombe O., Roure F., Lavé J., Vergés J. (eds) *Thrust belts and foreland basins. Frontiers in earth sciences*. Springer, Berlin, Heidelberg, https://doi.org/10.1007/978-3-540-69426-7_16
- Callot, J.-P., Trocmé, V., Letouzey, J., Albouyi, E., Jahani, S., Sherkati, S., 2012. Pre-existing salt structures and the folding of the Zagros Mountain, in G. I. Alsop, S. G. Archer, A. J. Hartley, N. T. Grant, and R. Hodgkinson, eds., *Salt tectonics, sediments and prospectivity: Geological Society, London, Special Publications 2012*, v. 363, p. 545–561, <http://dx.doi.org/10.1144/SP363.27>.
- Callot, J.-P., Salel, J.-F., Letouzey, J., Daniel, J.-M., Ringenbach, J.-C., 2016. Three-dimensional evolution of salt-controlled minibasins: Interactions, folding, and megaflop development. *AAPG Bulletin*, 100(9), 1419–1442. <http://dx.doi.org/10.1306/0310161408>.
- Cámara, P., 2017. Salt and Strike-Slip Tectonics as Main Drivers in the Structural Evolution of the Basque-Cantabrian Basin, Spain, Editor(s): Juan I. Soto, Joan F. Flinch, Gabor Tari, *Permo-Triassic Salt Provinces of Europe, North Africa and the Atlantic Margins*, Elsevier, Chapter 17, 371-393, <https://doi.org/10.1016/B978-0-12-809417-4.00018-5>.

- Canérot, J., Hudec, M. R., Rockenbauch, K., 2005. Mesozoic diapirism in the Pyrenean orogen: Salt tectonics on a transform plate boundary. *AAPG Bulletin*, 89(2), 211–229. <https://doi.org/10.1306/09170404007>.
- Caron, J.P., 1970. Episodes volcaniques et volcano-détritiques dans le Trias moyen de la partie méridionale de l'arc de Barjols (Var). *Comptes rendus de l'Académie des Sciences, Paris*, 270, D, 12231226.
- Caron, J.P., 1979. Trias au sud de l'Argens (Var). In Rouire et al., *Notice géologique de la feuille Brignoles à 1/50.000*, 6-7.
- Casagrande, L., Andrieux, J., Morel, J. L., 1989. Le massif de Suzette (Vaucluse): L'inversion tectonique d'un graben oligocène, *Géol. Fr.*, 3, 3–12.
- Cassini G., Durand, M., Ronchi, A., 2003. Permian-Triassic continental sequences of northwest Sardinia and south Provence: Stratigraphic correlations and palaeogeographical implications, *Boll. Soc. Geol. It.*, 2, 119–129.
- Cherchi, A., Mancin, N., Montadert, L., Murru, M., Terasa Putzu, M., Schiavinotto, F., Verrubbi, V., 2008. Les conséquences stratigraphiques de l'extension oligo-miocène en Méditerranée occidentale à partir d'observations dans le système de grabens de Sardaigne (Italie), *Bull. Soc. Géol. Fr.*, 179, 267–287.
- Clauzon, G., 1984. Evolution géodynamique d'une montagne provençale et de son piedmont ; l'exemple du Luberon (Vaucluse, France). *Montagnes et Piémonts, Toulouse, R.G.P.S.O.*
- Clauzon, G., Suc, J.-P., Gautier, F., Berger, A., Loutre, M.-F., 1996. Alternate interpretation of the Messinian salinity crisis: Controversy resolved? *Geology*, 24, 363–366, [http://dx.doi.org/10.1130/0091-7613\(1996\)024<0363:AIOTMS>2.3.CO;2](http://dx.doi.org/10.1130/0091-7613(1996)024<0363:AIOTMS>2.3.CO;2).
- Cornet, C., 1957. Etude tectonique et morphologique de la région de Méounes et de La Roquebrussanne. *Revue de Géographie physique et de Géologie dynamique (2)*, I, fasc.2, 113-118 et fasc. 4, 233-242.
- Cornet, C., 1965. Evolution tectonique et morphologique de la Provence depuis l'Oligocène *Mémoires de la Société géologique de France*, XLIV, fasc. 2., n° 103, 1-252, Pl. I-XI.
- Cornet, C., 1967. Le massif de Saint-Clément : conséquences de sa mise en place sur le Trias du Gapeau et de Garéoult ainsi que sur les massifs environnants. *Bull. Soc. Géol. de France*, 7, 579-584.
- Cornet, C., 1970. Sur les bandes triasiques provençales et les grabens qui leur sont liés. Leur parenté avec les grands rifts oligocènes. *Revue de Géographie physique et de Géologie dynamique*, XII, 1, 35-39.
- Corroy, G., 1957. La Montagne Sainte-Victoire. *Bulletin du Service de la Carte géologique de la France*, LV, n° 251, p. 1-46.
- Coward, M., Stewart, S., 1995. Salt influence structures in the Mesozoic-Tertiary cover of the Southern North Sea, U.K., in M. P. A. Jackson, D. G. Roberts, and S. Snelson, eds., *Salt tectonics: A global perspective: AAPG Memoir 65*, p. 229–250.
- Crévola, G., Pupin, J.-P., 1994. Crystalline Provence: structure and Variscan evolution. In: *Pre-Mesozoic geology in France and related areas*. Springer, Berlin Heidelberg, 426-441.
- Cushing, E. M., Bellier, O., Nechtschein, S., Sébrier, M., Lomax, A., Volant, P., Dervin, P., Guignard, P., Bove, L., 2008. A multidisciplinary study of a slow-slipping fault for seismic hazard assessment: The example of the Middle Durance Fault (SE France), *Geophys. J. Int.*, 172, 1163–1178, <http://dx.doi.org/10.1111/j.1365-246X.2007.03683.x>.

- Dahlstrom, C. D. A., 1969. Balanced cross-sections, *Can. J. Earth Sci.*, 6(4), 743–757.
- Dardeau, G., de Granciansky, P.-C., 1990. Halocinèse et rifting téthysien dans les Alpes-Maritimes (France). – *Bull. Cent. Rech. Explor. Prod. Elf Aquitaine*, 14, 443-464.
- Davis, D. M., Engelder, T., 1985. The role of salt in fold-and-thrust belts, *Tectonophysics*, 119, 67-88, [http://dx.doi.org/10.1016/0040-1951\(85\)90033-2](http://dx.doi.org/10.1016/0040-1951(85)90033-2)
- Delfaud, J., Toutin-Morin, N., Morin, R., 1989. Un cône alluvial en bordure d'un bassin intramontagneux: La formation permienne du Rocher de Roquebrune (Bassin du Bas-Argens, Provence orientale), *C. R. Acad. Sci., Ser. II: Mec., Phys., Chim., Sci. Terre Univers*, 309, 1811–1817.
- Duffy, O.B., Dooley, T.P., Hudec M.R., Jackson, M.P.A., Fernandez, N., Jackson, C.A-L., Soto, J.I., 2018. Structural evolution of salt-influenced fold-and-thrust belts: A synthesis and new insights from basins containing isolated salt diapirs, *Journal of Structural Geology*, 114, 206–221, <https://doi.org/10.1016/j.jsg.2018.06.024>.
- Durand, M., Gand, G., 2007. Le Permien et le Trias du Dôme de Barrot (Alpes-Maritimes) Livret-guide de l'excursion annuelle de l'Association des Géologues du Permien et du Trias, 18-20 Septembre 2007, 26p., <https://www.researchgate.net/publication/321293102>.
- Durand, J. P., Tempier, C., 1962. Etude tectonique de la zone des brèches du massif de Sainte-Victoire, dans la région du Tholonet, *Bull. Soc. Géol. Fr.*, 7, 97–101.
- Duvochel, P., Ferrandini, J., Laville, P., 1977. Lithologie et interprétation du sondage de Garéoult (Var) dans son cadre structural. *Bulletin du B.R.G.M.*, 2^e série, sect. 1, n° 4, 333-340.
- Eisenlohr, B., 1974a, Etude stratigraphique et structurale du massif de la Loube (Var). Thèse de spécialité, Université de Provence 145 p.
- Eisenlohr, B., 1974b. L'allochtonie du massif de la Loube (Var) et du Trias qui le borde. Conséquences structurales. *Comptes Rendus de l'Académie des Sciences, Paris*, 279, D, 731-734.
- Elliott, D., 1983. The construction of balanced cross sections, *J. Struct. Geol.*, 5, 101, [http://dx.doi.org/10.1016/0191-8141\(83\)90035-4](http://dx.doi.org/10.1016/0191-8141(83)90035-4).
- Emré, T., Truc, G., 1978. Mise en évidence d'un contact discordant Oligocène-Trias dans le massif de Suzette. Implications tectoniques et conséquences sur l'origine des évaporites ludiennes du bassin de Mormoiron (Vaucluse). *Géol. Alp.*, 54, 17-23.
- Espurt, N., Brusset, S., Baby, P., Hermoza, W., Bolanõs, R., Uyen, D., and Déramond, J., 2008. Paleozoic structural controls on shortening transfer in the Subandean foreland thrust system, Ene and southern Ucayali basins, Peru: *Tectonics*, v. 27, TC3009, <http://dx.doi.org/10.1029/2007TC002238>.
- Espurt, N., Hippolyte, J.-C., Saillard, M., Bellier, O., 2012. Geometry and kinematic evolution of a long-living foreland structure inferred from field data and cross section balancing, the Sainte-Victoire system, Provence, France: *Tectonics*, v. 31, p. TC4021, <http://dx.doi.org/10.1029/2011TC002988>.
- Fabre-Taxy, S., Philip, J., 1964. La zone du Plan d'Aups dans sa région type la Ste Baume. *Bulletin de la Société géologique de France*, VI, 4, 554-559.
- Ferrer O., Jackson M. P. A., Roca E., Rubinat M., 2012. Evolution of salt structures during extension and inversion of the Offshore Parentis Basin (Eastern Bay of Biscay), *Salt Tectonics, Sediments and Prospectivity*, G. I. Alsop, S. G. Archer, A. J. Hartley, N. T.

- Grant, R. Hodgkinson, Geological Society of London. Special Publication, 363, 361-379, <https://dx.doi.org/10.1144/SP363.16>.
- Floquet, M., Gari, J., Hennuy, J., Léonide, P., Philip, J., 2005. Sédimentations gravitaires carbonatées et silicoclastiques dans un bassin en transtension, séries d'âge cénoomanien à coniacien moyen du Bassin sud-provençal. *Publ. ASF*, 52, 80 p.
- Floquet, M., Philip, J., Léonide, P., Gari J., 2006. Sédimentation et géodynamique du bassin Sud-Provençal au Crétacé supérieur; Histoire et dynamique des plates-formes carbonatées et de leur biotas durant le Phanérozoïque. – Livret guide d'excursion géologique, Université de Provence, Marseille, 69 p. Livre en dépôt à la Soc. géol. France.
- Gharbi, M., Espurt, N., Masrouhi, A., Bellier, O., Amari E.A., 2015. Style of Atlassic tectonic deformation and geodynamic evolution of the southern Tethyan margin, Tunisia. *Marine and petroleum geology* 66, 801-816, <http://dx.doi.org/10.1016/j.marpetgeo.2015.07.020>.
- Giles, K.A., Rowan, M.G., 2012. Concepts in halokinetic-sequence deformation and stratigraphy, in G.I., Alsop, S.G., Archer, A.J., Hartley, N.T., Grant, R., Hodgkinson, eds., *Salt tectonics, sediments and prospectivity: Geological Society, London, Special Publications*, 363, 7–31, <http://dx.doi.org/10.1144/SP363.8>
- Godet, B., 1976. Etude stratigraphique et structurale de la partie occidentale du Massif de Bras et de ses bordures (Var). Thèse, Université de Provence, 89 p.
- Gouvernet, C., 1963. Structure de la région toulonnaise. *Mém. Carte Géol. Fr.*, 244 p., 6 pl.
- de Graciansky, P.-C., Lemoine, M., 1988. Early Cretaceous tectonics in the southwestern French Alps: a consequence of North-Atlantic rifting during Tethyan spreading. *Bull. Soc. géol. Fr.*, 8, IV, 5, 733-737.
- Graham, R., Jackson, M., Pilcher, R., Kilsdonk, W., 2012. Allochthonous salt in the sub-Alpine fold-thrust belt of Haute Provence, France: Geological Society, London, *Special Publications*, v. 363, 595–615, <http://dx.doi.org/10.1144/SP363.30>.
- Guieu, G., 1968. Etude tectonique de la région de Marseille. *Publications de l'Université de Provence*, 2 t., 604 p.
- Guyonnet-Benaize, C., Lamarche, J., Hollender, F., Viseur, S., Münch, P., Borgomano, J., 2015. Three-dimensional structural modeling of an active fault zone based on complex outcrop and subsurface data: The Middle Durance Fault Zone inherited from polyphase Meso-Cenozoic tectonics (southeastern France), *Tectonics*, 34, 265–289, <http://dx.doi.org/10.1002/2014TC003749>.
- Harding, R., Huuse, M., 2015. Salt on the move: Multi stage evolution of salt diapirs in the Netherlands North Sea. *Marine and Petroleum Geology*, 61, 39-55.
- Haug, E., 1925. Les nappes de charriages de la Basse Provence, 1 partie. La région toulonnaise. *Mém. Serv. Carte géol. Fr.*, 304 p.
- Hennuy, J., 2003. Sédimentation carbonate et silicoclastique sous contrôle tectonique, le bassin sud-provençal et sa plate-forme carbonatée du Turonien au Coniacien moyen. Evolution séquentielle, diagénétique, paléogéographique, Thèse Sci., 252 pp., Aix-Marseille Univ., Centre Saint-Charles, Marseille.
- Hibsch, C., Kandel, D., Montenat, C., Ott d'Estevou, P., 1992. Evénements tectoniques crétaqués dans la partie méridionale du bassin subalpin (massif Ventoux-Lure et partie occidentale de l'Arc de Castellane, SE France). Implications géodynamiques. *Bull. Soc. géol. Fr.*, 163, 2, 147-158.

- Hippolyte, J.-C., Angelier, J., Nury, D., Bergerat, F., Guieu, G., 1993. Tectonic-stratigraphic record of paleostress time changes in the Oligocene basins of the Provence, southern France, *Tectonophysics*, 226, 15–35, [http://dx.doi.org/10.1016/0040-1951\(93\)90108-V](http://dx.doi.org/10.1016/0040-1951(93)90108-V).
- Hudec M.R., Jackson, M.P.A., 2009. Interaction between spreading salt canopies and their peripheral thrust system. *J. Struct. Geol.*, 31, 1114-1129.
- Huyghe, P., Mascle, G., Faucher, T., 1999. Témoins structuraux et géochimiques de diapirs syncriés dans les Alpes Occidentales, *Géologie Alpine*, 75, 111-116.
- Jackson, M.P.A., Vendeville, B.C., 1994. Regional extension as a geological trigger for diapirism. *Geol. Soc. Am. Bull.* 106, 57-73.
- Jahani, S., Callot, J.-P., Letouzey, J., Frizon de Lamotte, D., 2009. The eastern termination of the Zagros Fold-and-Thrust Belt, Iran: Structures, evolution, and relationships between salt plugs, folding, and faulting, *Tectonics*, 28, TC6004, <http://dx.doi.org/10.1029/2008TC002418>.
- Jannin, S., 2011. Rôle de la tectonique salifère dans la structuration du bassin du Sud-Est (SE de la France): Définition d'un modèle de tectonique salifère d'après l'étude du secteur de Draguignan et comparaison de ce modèle aux structures halocinétiques rencontrées sur l'ensemble du bassin, *Mém. d'Ing. Géol.*, n° 476, 97 pp., 50 fig., 4 annexes, Inst. Polytech Lasalle Beauvais, Beauvais, France.
- Kergaravat, C., Ribes, C., Legeay, E., Callot, J.-P., Kavak, K. S., Ringenbach, J.-C., 2016. Minibasins and salt canopy in foreland fold-and-thrust belts: The central Sivas Basin, Turkey, *Tectonics*, 35, 1342–1366, <http://dx.doi.org/10.1002/2016TC004186>.
- Lacombe, O., Angelier, J., Laurent, P., 1992. Determining palaeostress orientations from faults and calcite twins: A case study near the Sainte-Victoire Range (southern France), *Tectonophysics*, 201, 141–156, [http://dx.doi.org/10.1016/0040-1951\(92\)90180-E](http://dx.doi.org/10.1016/0040-1951(92)90180-E).
- Lacombe, O., Mouthereau, F., 2002. Basement involved shortening and deep detachment tectonics in forelands of orogens: Insights from recent collision belts (Taiwan, Western Alps, Pyrenees), *Tectonics*, 21(4), 1030, <http://dx.doi.org/10.1029/2001TC901018>.
- Lacombe O., Jolivet L., 2005. Structural and kinematic relationships between Corsica and the Pyrenees-Provence domain at the time of the Pyrenean orogeny. *Tectonics*, 24, TC 1003, <http://dx.doi.org/10.1029/2004TC001673>.
- Lacombe, O., Bellahsen, N., 2016. Thick-skinned tectonics and basement-involved fold–thrust belts: insights from selected Cenozoic orogens. *Geological Magazine*, 153(5/6), 763–810. <http://dx.doi.org/10.1017/S0016756816000078>.
- Lagabrielle, Y., Labaume, P., de Saint Blanquat, M., 2010. Mantle exhumation, crustal denudation, and gravity tectonics during Cretaceous rifting in the Pyrenean realm (SW Europe): Insights from the geological setting of the lherzolite bodies. *Tectonics*, 29, TC4012. <http://dx.doi.org/10.1029/2009TC002588>.
- de Lapparent, A.-F., 1938a. Etudes de paléontologie stratigraphique sur les faunes continentales de Provence. *Mémoire de la Société géologique de France*, n.s. 15 35, 1–34.
- de Lapparent, A.-F., 1938b. Etudes géologiques dans les Régions Provençales et Alpines entre le Var et la Durance. *Bulletin de la Carte Géologique de la France*, 40, 198, 1-302.
- Laville, P., 1981. La formation bauxitique provençale (France). Séquence des faciès chimiques et paléomorphologie Crétacée. *Chronique de la recherche minière*, 462, 51-68.

- Leleu, S., Ghienne, J.-F., Manatschal, G., 2005. Upper Cretaceous-Palaeocene basin margin alluvial fans documenting interaction between tectonic and environmental processes (Provence, SE France), *Geol. Soc. Spec. Publ.*, 251, 217–239.
- Lemoine, M., de Graciansky, P.-C., 1988. Histoire d'une marge continentale passive: les Alpes occidentales au Mésozoïque. Introduction. *Bull. Soc. géol. Fr.*, 8, V, 597-600.
- Léonide, P., 2007. Réponses des plates-formes carbonatées aux changements paléoocéanographiques, paléo-climatiques et tectoniques: le bassin sud-provençal au jurassique inférieur à moyen. Thèse de Doctorat de l'Université de Provence, Marseille, 385 p.
- Léonide, P., Floquet, M., Villier, L., 2007. Interaction of tectonics, eustasy, climate and carbonate production on the sedimentary evolution of an Early/Middle Jurassic extensional basin (southern Provence Sub-basin, SE France). *Basin Res.*, 19, 1, 125-152.
- Léonide, P., Borgomano, J., Masse, J.-P., Doublet, S., 2012. Relation between stratigraphic architecture and multi-scale heterogeneities in carbonate platforms: The Barremian-lower Aptian of the Monts de Vaucluse, SE France, *Sediment. Geol.*, 265–266, 87–109, <http://dx.doi.org/10.1016/j.sedgeo.2012.03.019>.
- Le Pichon, X., Rangin, C., Hamon, Y., Loget, N., Lin, J.Y., Andreani, L., Flotte, N., 2010. Geodynamics of the France Southeast Basin, *Bull. Soc. Géol. Fr.*, 181, 477–501, <http://dx.doi.org/10.2113/gssgfbull.181.6.477>.
- López-Mir, B., Anton Muñoz, J., García Senz, J., 2014. Restoration of basins driven by extension and salt tectonics: Example from the Cotiella Basin in the central Pyrenees. *Journal of Structural Geology*, 69, 147–162. <https://doi.org/10.1016/j.jsg.2014.09.022>.
- Machhour, L., Philip, J., Oudin, J.L., 1994. Formation of laminate deposits in anaerobic-dysaerobic marine environments. *Marine Geology*, 117, 287-302.
- Masclé, G., Arnaud, H., Dardeau, G., Debelmas, J., Delpech, P.-Y., Dubois, P., Gidon, M., de Graciansky, P.-C., Kerkhove, C., Lemoine, M., 1988. Salt tectonics, Tethyan rifting and Alpine folding in the French Alps. *Bull. Soc. géol. Fr.*, (8), IV, 747-758.
- Masse, J.-P., Philip, J., 1976. Paléogéographie et tectonique du Crétacé moyen en Provence, *Rev. Geogr. Phys. Geol. Dyn.*, 2, 49–66.
- Masse, J.-P., Villeneuve, M., Léonforte, E., Nizou, J., 2009. Block tilting of the North Provence Early Cretaceous carbonate margin; stratigraphic, sedimentologic and tectonic data. *Bull. Soc. géol. Fr.*, 180, 2, 105-115.
- Masse, J.-P. Fenerci-Masse, M., 2013. Drowning events, development and demise of carbonate platforms and controlling factors: the Late Barremian – Early Aptian record of Southeast France. *Sedim. Geol.*, 298, 28-52.
- Ménard, G., 1980. Profondeur du socle antétriasique dans le Sud-Est de la France, *C. R. Acad. Sci. Paris*, 290, 299–302.
- Mennessier, G., 1959a. Etude tectonique des confins alpino-provençaux entre le Verdon et l'Argens. *Mémoires de la Société géologique de France*, XXXVIII, 4, n° 87, 174 p., VIII pl.
- Mennessier, G., 1959b. Etude tectonique du massif de la Loube (Var). *Bulletin de la Société géologique de France*, (7), I, 43-51.
- Mennessier, G., Modret D., 1966. Carte géologique détaillée de la France à 1/50 000 : Tavernes. Paris : Service de la carte géologique de France, 996, carte et notice explicative.

- Mennessier, G., de Lapparent, A.-F., Bordet, P., 1969. Carte géologique détaillée de la France à 1/50 000 : Draguignan. 2^{ème} édition. Orléans : BRGM, 1023, carte et notice explicative.
- Mennessier, G., 1975. Etude tectonique du massif de Bras (Var) et description détaillée des synclinaux bauxitifères à partir des travaux miniers (feuilles de Draguignan et de Brignoles à 1/50.000) Bulletin du B.R.G.M., 2^e série, n°3, 183-213.
- Muñoz, J.A., 1992. Evolution of a continental collision belt: ECORS-Pyrenees crustal balanced cross-section. In Thrust Tectonics, Mc Clay, K. (Ed), Chapman and Hall, London, 235–246.
- Nalpas, T., Brun, J.-P., 1993. Salt flow and diapirism related to extension at crustal scale: Tectonophysics, v. 228, p. 349–362, [http://dx.doi.org/10.1016/0040-1951\(93\)90348-N](http://dx.doi.org/10.1016/0040-1951(93)90348-N).
- Nury, D., 1988. L'Oligocène de Provence méridionale. Stratigraphie, dynamique sédimentaire, reconstitutions paléogéographiques. Doc. BRGM, 163, 411 p. Thèse Sci., 1987, Université de Provence, Marseille.
- Onézime, J., Faure, M., Crévola, G., 1999. Étude pétro-structurale du complexe granitique Rouet – Plan-de-la-Tour (massifs des Maures et du Tanneron occidental, Var). C. R. Acad. Sci., Paris, (IIA), 328, 11, 773-779.
- Peel, F.J., 2014. How do salt withdrawal minibasins form? Insights from forward modelling, and implications for hydrocarbon migration, Tectonophysics, 630, 222–235, <http://dx.doi.org/10.1016/j.tecto.2014.05.027>.
- Philip, J., 1965. Nouvelles observations sur la structure du synclinal du Plan d'Aups dans le massif de la Sainte-Baume. Compte rendu sommaire des séances de la Société géologique de France, 310-312.
- Philip, J., 1967. Modalités et importance de la transgression du Sénonien inférieur dans la région de Saint-Cyr-sur-Mer (Var). C. R. Acad. Sci., Paris, 265, 1883-1886.
- Philip, J., 1970. Les formations calcaires à rudistes du Crétacé supérieur provençal et rhodanien. Thèse Sci., Université de Provence, Marseille, 438 p.
- Philip, J., Masse, J.-P., Machhour, L., 1987. L'évolution paléogéographique et structurale du front de chevauchement nord-toulonnais (Basse-Provence occidentale, France), Bull. Soc. Géol. Fr., 8(III), 541–550.
- Philip, J., Vianey-Liaud, M., Martin-Closas, C., Tabuce, R., Léonide, P., Margerel, J. P., Noël, J., 2017. Stratigraphy of the Haut Var Paleogene continental series (Northeastern Provence, France): New insight on the age of the 'Sables bleutés du Haut Var' Formation. Geobios, 50(4), 319-339.
- Philip, J., 2012. L'exploration géologique de la Provence: deux siècles et demi de débats et de controverses. Presses des Mines, Collection Histoire Sciences et sociétés, 366 p.
- Philip, J., 2018a. La bande triasique de l'Huveaune, in Villeneuve et al., Mémoire explicatif, Carte géol. France (1/50 000), feuille Aubagne-Marseille, 3^{ème} édition (1044), 148-156.
- Philip, J., 2018b. La série sédimentaire d'âge céno-manien à maastrichtien du massif de la Ste Baume, in Villeneuve et al., Mémoire explicatif, Carte géol. France (1/50 000), feuille Aubagne-Marseille, 3^{ème} édition (1044), 77-80.
- Popoff, M., 1973. La bande triasique de Barjols (Var) : la bordure sud-occidentale. Thèse de 3^e cycle, Université de Paris VI, 160 p.

- Rolland, Y., Corsini, M., Demoux, A., 2009. Metamorphic and structural evolution of the Maures-Tanneron massif (SE Variscan chain): Evidence of doming along a transpressional margin, *Bull. Soc. Geol. Fr.*, 180, 217–230, <http://dx.doi.org/10.2113/gssgfbull.180.3.217>.
- Roure, F., Colletta, B., 1996. Cenozoic inversion structures in the foreland of the Pyrenees and Alps, in *Peri-Tethys Memoir 2: Structure and Prospects of Alpine Basins and Forelands*, *Mem. du Mus. Natl. Hist. Nat.* 170, edited by P. A. Ziegler, 173–209, Mus. Natl. Hist. Nat., Paris.
- Roure, F., Brun, J.-P., Colletta, B., Van Den Driessche, J., 1992. Geometry and kinematics of extensional structures in the alpine foreland basin of southeastern France, *J. Struct. Geol.*, 14, 503–519, [http://dx.doi.org/10.1016/0191-8141\(92\)90153-N](http://dx.doi.org/10.1016/0191-8141(92)90153-N).
- Rowan, M.G., Vendeville, B.C., 2006. Foldbelts with early salt withdrawal and diapirism: Physical model and examples from the northern Gulf of Mexico and the Flinders Ranges, *Australia: Marine and Petroleum Geology*, v. 23, no. 9–10, p. 871–891, <http://dx.doi.org/10.1016/j.marpetgeo.2006.08.003>.
- Rowan, M.G., Giles, K.A., Hearon IV, T.E., Fiduk, J.C., 2016. Megaflaps adjacent to salt diapirs. *AAPG Bulletin*, 100, 1723–1747.
- Saura, E., Vergés, J., Martin-Martin, J.D., Messenger, G., Moragas, M., Razin, P., Grelaud, C., Jousseaume, R., Malaval, M., Homke, S., Hunt, D.W., 2014. Syn- to post-rift diapirism and minibasins of the Central High Atlas (Morocco): the changing face of a mountain belt. *J. Geol. Soc.* 171, 97-105.
- Saura, E., Ardèvol i Oró, L., Teixell, A., Vergés, J., 2016. Rising and falling diapirs, shifting depocenters, and flap overturning in the Cretaceous Sopeira and Sant Gervàs subbasins (Ribagorça Basin, southern Pyrenees), *Tectonics*, 35, 638–662, <http://dx.doi.org/10.1002/2015TC004001>.
- Shaw, J., Connors, C., Suppe, J., 2005. Seismic interpretation of contractional fault-related folds, in *AAPG Seismic Atlas*, *Stud. Geol.*, vol. 53, pp. 1–156, Am. Assoc. of Pet. Geol., Tulsa, Okla.
- Schettino, A., Turco, E., 2011. Tectonic history of the western Tethys since the Late Triassic, *Geol. Soc. Am. Bull.*, 123, 89–105, <http://dx.doi.org/10.1130/B30064.1>.
- Schönborn, G., 1992. Kinematics of a transverse zone in the Southern Alps, Italy, In *Thrust Tectonics*, Mc Clay, K. (Ed), Chapman and Hall, London, 299-310.
- Sherkati, S., Letouzey, J., Frizon de Lamotte, D., 2006. Central Zagros fold-thrust belt (Iran): New insights from seismic data, field observation, and sandbox modeling, *Tectonics*, 25, TC4007, <http://dx.doi.org/10.1029/2004TC001766>.
- Tavani, S., Bertok, C., Granado, P., Piana, F., Salas, R., Vigna, B., Muñoz, J.A., 2018. The Iberia-Eurasia plate boundary east of the Pyrenees, *Earth-Science Reviews*, <https://doi.org/10.1016/j.earscirev.2018.10.008>.
- Teixell, A., Barnolas, A., Rosales, I., Arboleya, M.-L., 2017. Structural and facies architecture of a diapir-related carbonate minibasin (lower and middle Jurassic, High Atlas, Morocco), *Marine and Petroleum Geology*, 81, 334-360, <https://doi.org/10.1016/j.marpetgeo.2017.01.003>.
- Tempier, C., 1987. Modèle nouveau de mise en place des structures provençales, *Bull. Soc. Geol. Fr.*, 8, 533–540.

- Thiele, R., 1972. De la Sainte-Baume au Roc de Candelon : contribution à l'étude géologique du chevauchement sud-provençal. Thèse de spécialité, Université Paris VI, 333p.
- Touraine, F., 1978. Le fossé de Montmeyan. Bulletin du BRGM, 2^{ème} série, section 1, N°2, 89-109.
- Toutin-Morin, N., Bonijoly, D., 1992. Structuration des bassins de Provence orientale à la fin de l'ère primaire, Cuad. Geol. Iber., 16, 59–74.
- Toutin-Morin, N., Bonijoly, D., Brocard, C., Dardeau, G., Dubar, M., 1992. Rôle des structures tardi à post-hercyniennes dans l'évolution de la plate-forme provençale (bordure des Maures et du Tanneron, France). C. R. Acad. Sci., Paris, 315, 1725-1732.
- Toutin-Morin, N., Bonijoly, D., Brocard, C., Dardeau, G., Dubar, M., 1993. Enregistrement sédimentaire de l'évolution post-hercynienne, en bordure des Maures et du Tanneron, du Carbonifère supérieur à l'Actuel. Géologie de la France, n° 2, 3-22.
- Toutin-Morin, N., Bonijoly, D., Brocard, C., Broutin, J., Crévola, G., Dardeau, G., Dubar, M., Féraud, J., Giraud, J.D., Godefroy P., Laville, P., Meinesz, A., 1994. Carte géologique de la France à 1/50.000. Fréjus- Cannes 2^e édition. Notice explicative, 187 p.
- Trusheim, F., 1960. Mechanism of salt migration in northern Germany. Am. Assoc. Pet. Geol. Bull. 44, 1519–1540.
- Turienzo, M., Sánchez, N., Dimieri, L., Lebinson, F., Araujo, V., 2014. Tectonic repetitions of the Early Cretaceous Agrio Formation in the Chos Malal fold-and-thrust belt, Neuquén Basin, Argentina: Geometry, kinematics and structural implications for Andean building, Journal of South American Earth Sciences, 53, 1-19, <https://doi.org/10.1016/j.jsames.2014.04.004>.
- Vergés, J., Millan, H., Roca, E., Muñoz, J.A., Marzo, M., Cirés, J.,...,1995. Eastern Pyrenees and related foreland basins: Pre-, syn- and post-collisional crustal-scale cross-sections. Marine and Petroleum Geology, 12(8), 893–915.
- Villeger, M., Andrieux, J., 1987. Phases tectoniques post-éocènes et structuration polyphasée du panneau de couverture nord provençal (Alpes externes méridionales), Bull. Soc. Géol. Fr. III, 8(1), 147–156.
- Warsitzka, M., Kley, J., Kukowski, N., 2015. Analogue experiments of salt flow and pillow growth due to basement faulting and differential loading. Solid earth.. 6, 9-31, <https://doi.org/10.5194/se-6-9-2015>.
- Westphal, M., Durand, J.P., 1990. Magnétostratigraphie des séries continentales fluvio-lacustres du Crétacé supérieur dans le synclinal de l'Arc (région d'Aix-en-Provence, France). Bulletin de la Société Géologique de France, (8), VI, n° 4, 609-620.
- Worrall, D.M., Snelson, S., 1989. Evolution of the northern Gulf of Mexico, with emphasis on Cenozoic growth faulting and the role of salt. In: Bally, A.W., Palmer, A.R. (Eds.), The Geology of North America: An overview: Boulder, Colorado. Geological Society of America, Geology of North America, v. A, pp. 97–138.
- Zürcher, P., 1893. Note sur les phénomènes de recouvrement des environs de Toulon. Bull. Soc. géol. Fr., 3, XXI, 65-77.

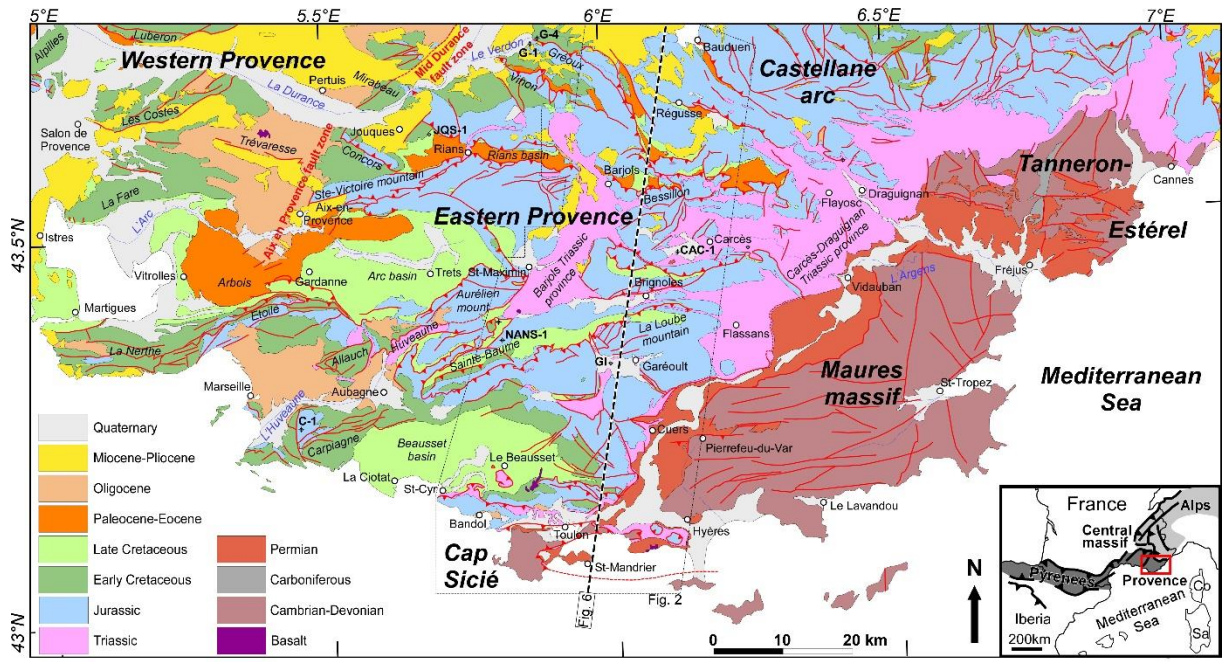


Fig. 1: Geodynamic setting of the Provence fold-thrust belt. Co: Corsica. Sa: Sardinia.

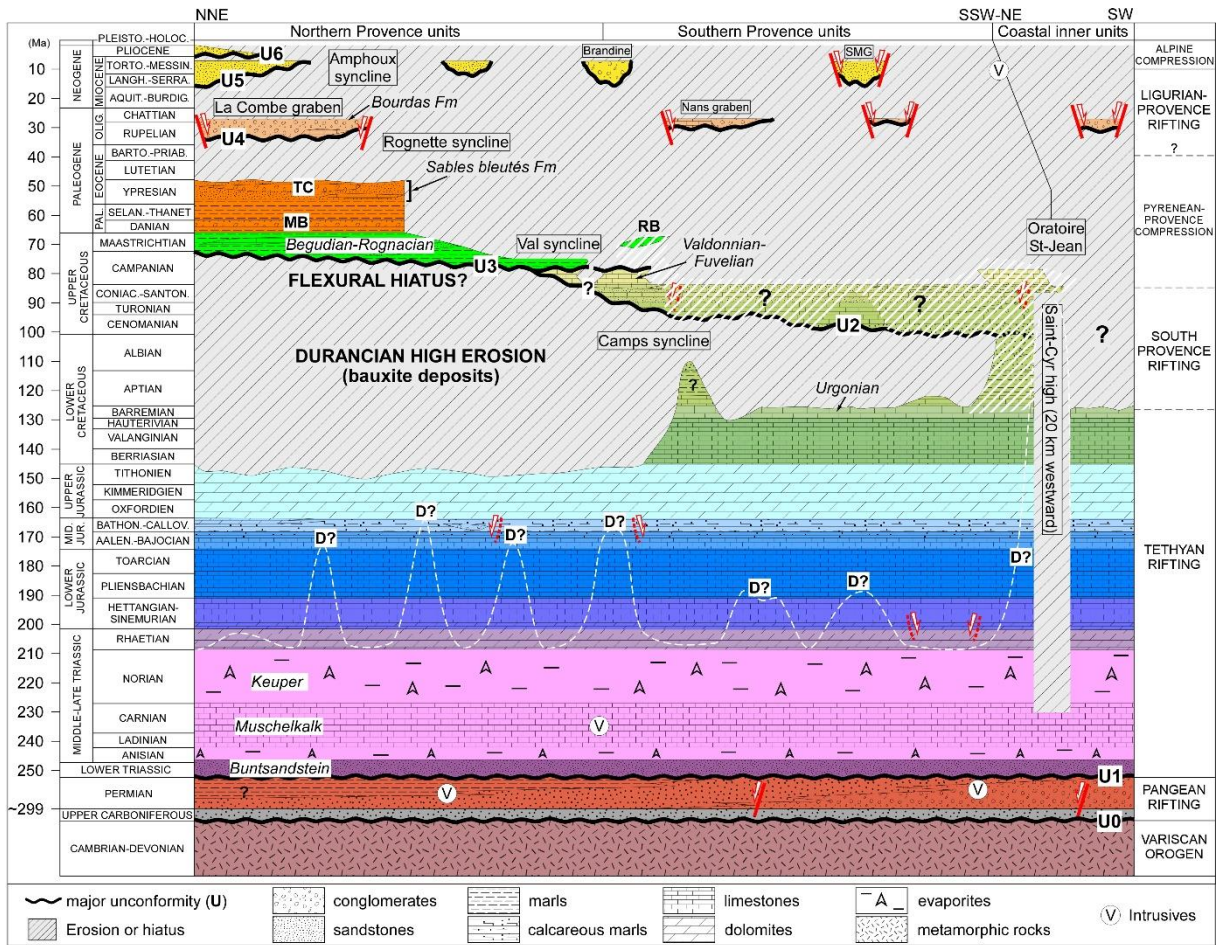


Fig. 3: Stratigraphy of the eastern Provence basin. Dashed area in southern Provence units corresponds to westerly outcrops in the Beausset syncline and Sainte-Baume thrust. RB: Rognacian breccias. MB: Microcodium breccias. TC: Touars conglomerates. SMG: Signes-Méounes graben. Dashed white lines indicates the inferred diapires (D).

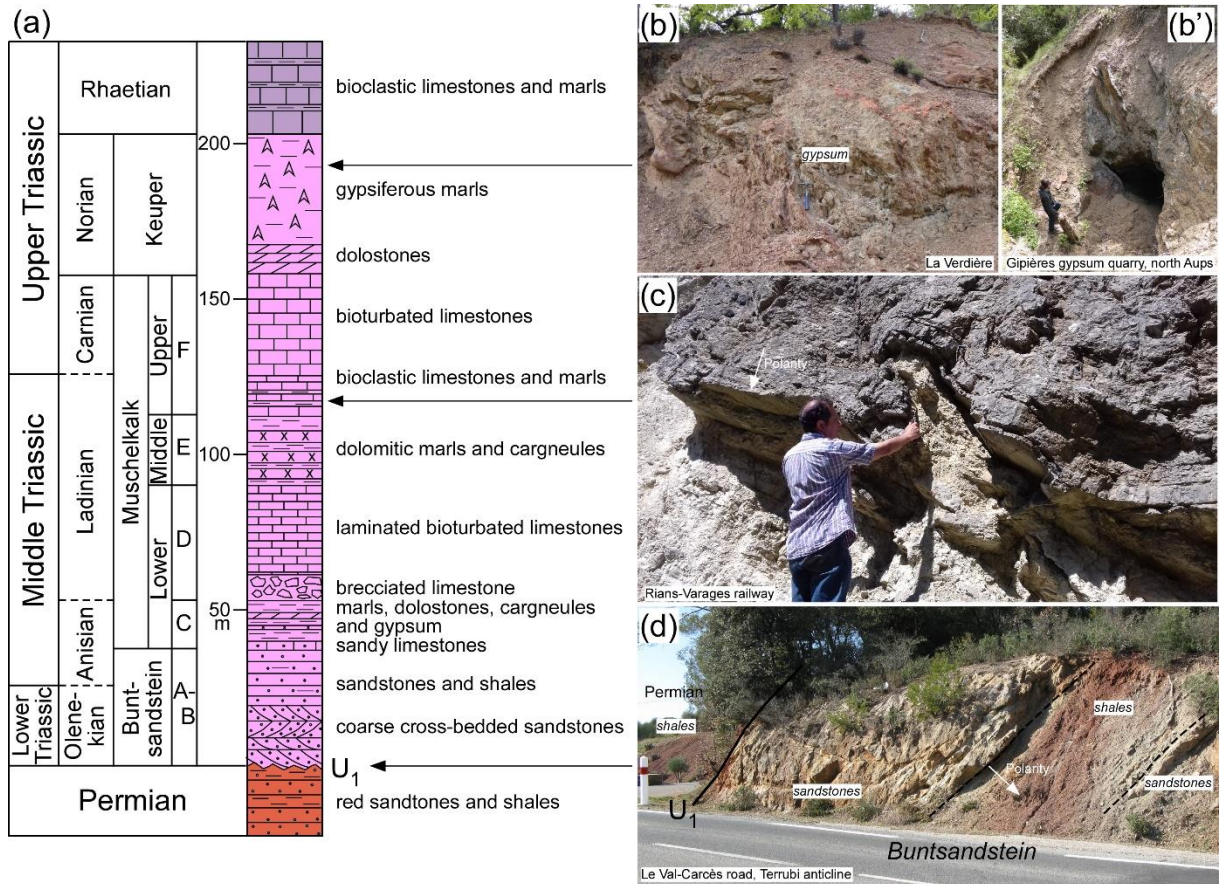
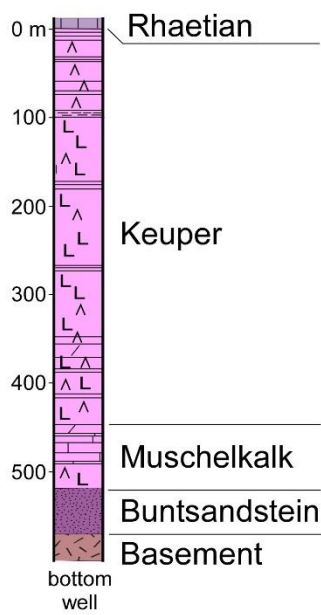
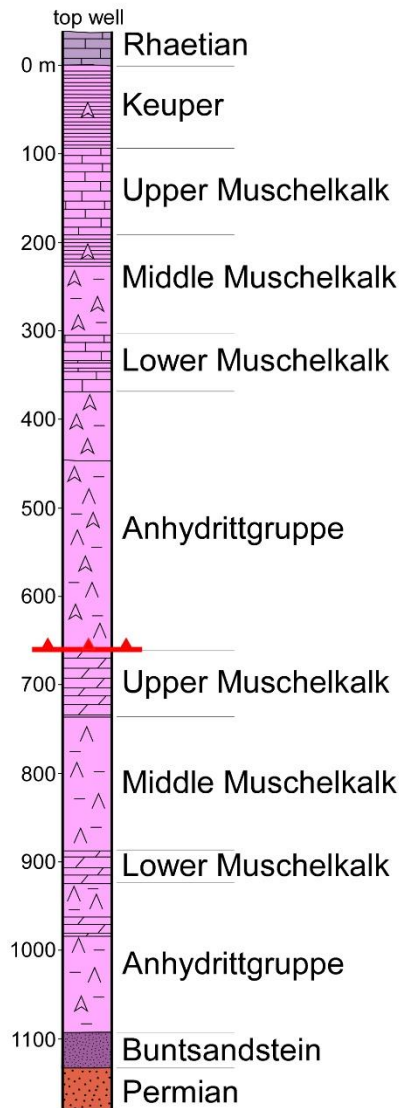


Fig. 4: Stratigraphic standard section of the Trias rocks in the eastern Provence (after Brocard and Philip 1989, Brocard, 1991 and Toutin-Morin et al. 1994; modified). (b) and (b'): Gypsum layers in Keuper near La Verdrière and Aups towns, respectively. (c): Muschelkalk limestones near Varages town. (d): Buntsandstein and Permian rocks in the Terrubi anticline.

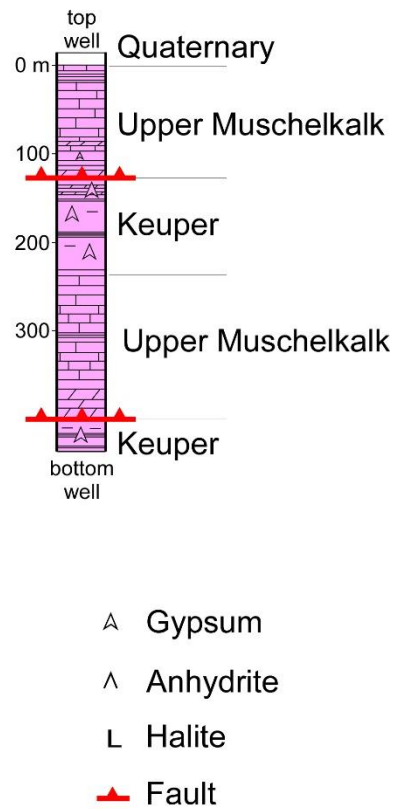
Jouques-1 (JQS-1)



Carcès-1 (CAC-1)



Garéoult (GI)



- △ Gypsum
- ∧ Anhydrite
- L Halite
- ▲ Fault

Fig. 5: Subsurface data from the Jouques-1, Carcès-1 and Garéoult exploration wells showing the thickness variations of the middle-upper Triassic evaporitic-carbonate strata. For locations, see Figs. 1 and 2.

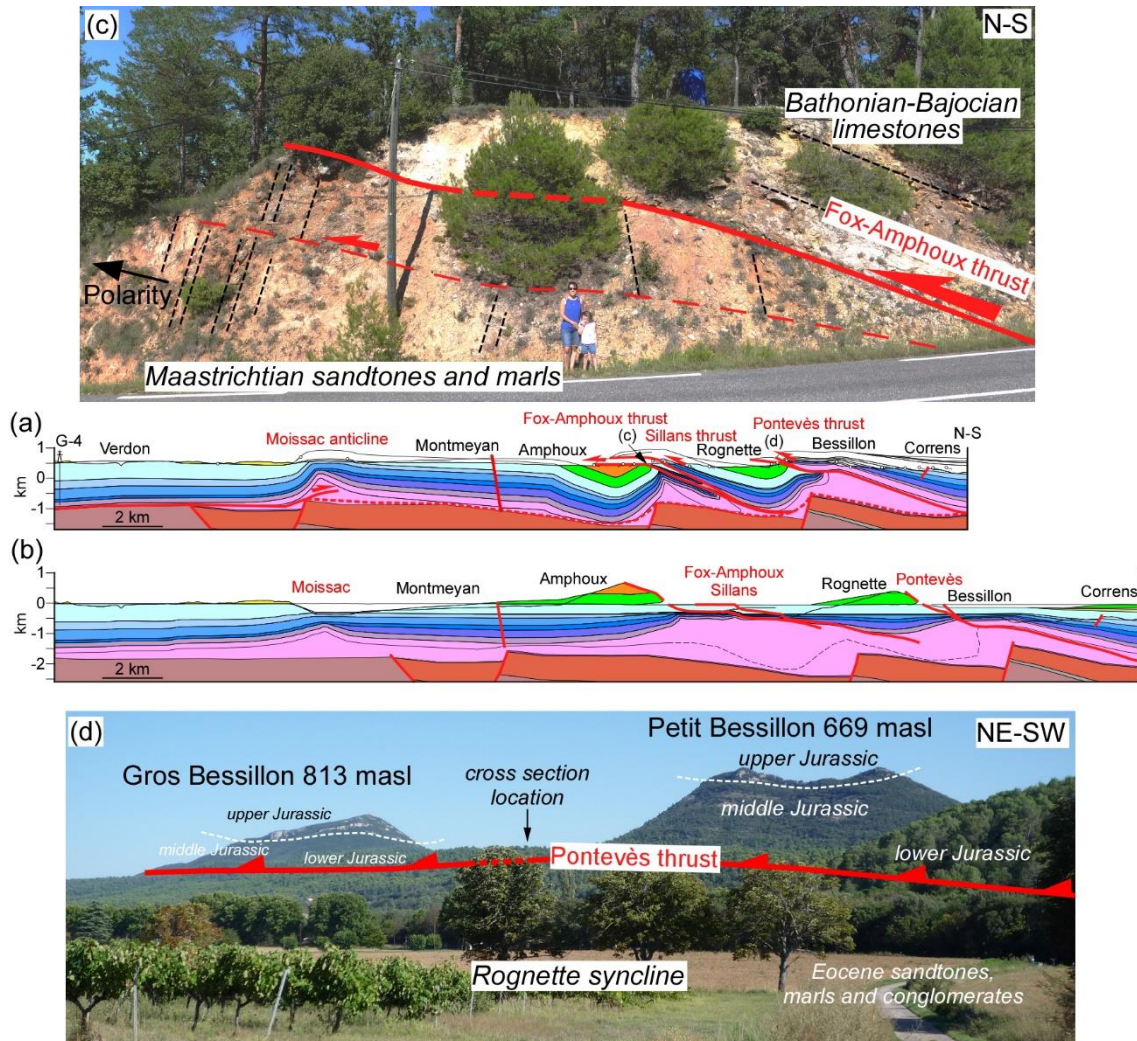


Fig. 7: (a) Structure and (b) restoration of the northern thrust systems (Moissac anticline, Fox-Amphoux/Sillans thrust system, and Pontevès thrust system). Horizon depth under the Verdon region is calibrated using the Gréoux-4 well (G-4). Structures referred to in the text are labeled. For legend, see Fig. 6. (c) View of the north-verging Fox-Amphoux thrust (and associated minor footwall thrust) placing Bathonian-Bajocian limestones on steep north-dipping Maastrichtian sandstones of the Amphoux syncline (see location in Fig. 2). (d) Panoramic view looking south-eastward of the Pontevès thrust transporting the Bessillon perched synclines above Ypresian strata of the Rognette syncline (see location in Fig. 10a). Note that the cross section trace is located eastward between the Bessillon synclines.

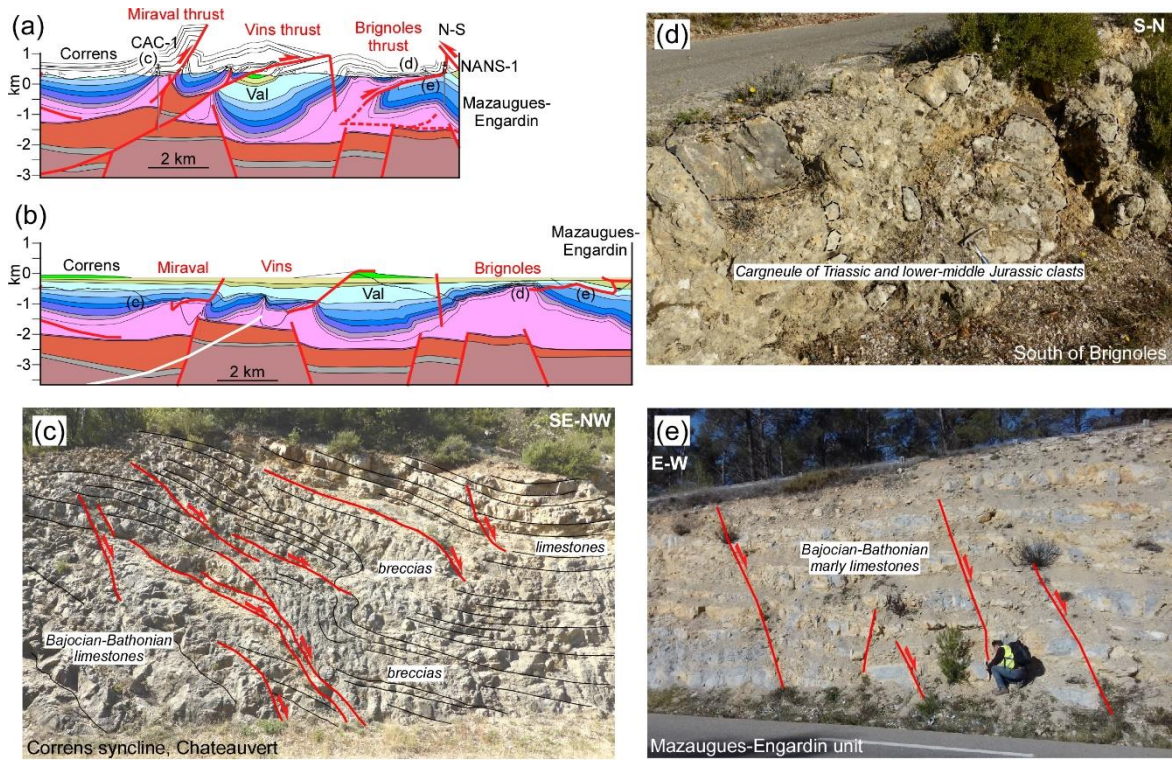


Fig. 8: (a) Structure and (b) restoration of the south-verging Bras imbricate. The geometry at depth is calibrated using the Carcès-1 (CAC-1) and Nans-les-Pins (NANS-1) wells. Structures referred to in the text are labeled. For legend, see Fig. 6. (c) NW-directed gravitational instabilities in the Bathonian-Bajocian limestones of the southern limb of the Correns syncline. (d) Residual middle Jurassic cap-rock or salt canopy (breccia-cargneule of Triassic and lower-middle Jurassic clasts) overlying Triassic evaporites in the Brignoles anticline. (e) NE-trending extensional faulting in Bajocian-Bathonien marly limestones. For locations, see Fig. 10a.

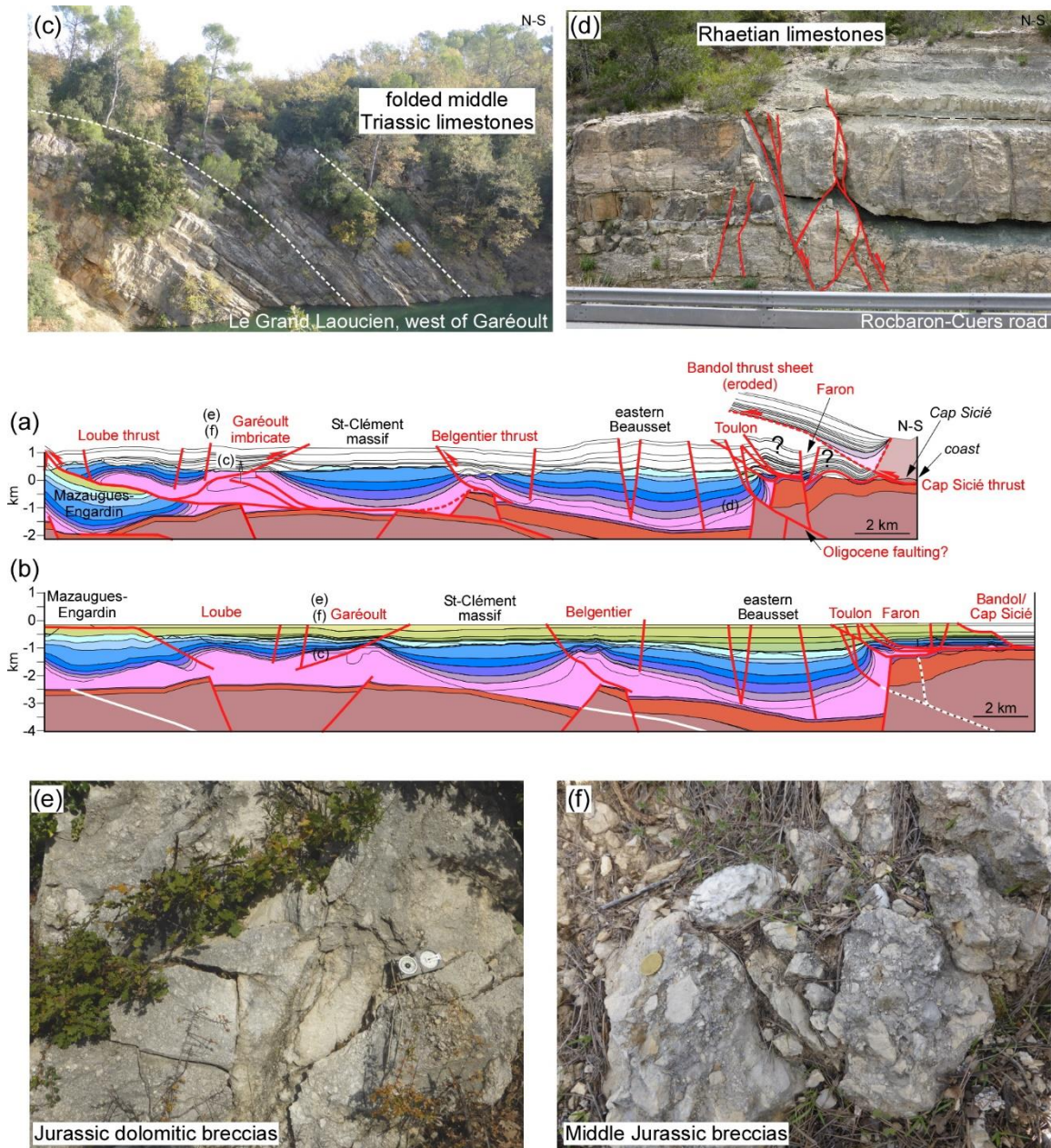


Fig. 9: (a) Structure and (b) restoration of the southern thrust systems (Loube thrust, Garéoult imbricate, Belgentier, Toulon, Faron, Bandol, Cap Sicié). Structures referred to in the text are labeled. For legend, see Fig. 6. (c) Disharmonic folding in middle Triassic limestones, northern flank of the Garéoult diapir (see location in Fig. 10b). (d) Syn-sedimentary normal faulting in Rhaetian limestones of the eastern Beausset syncline (see location in Fig. 10b). (e) and (f): Middle-upper Jurassic breccia deposits in the northern flank of the Garéoult diapir (east of Garéoult town) above Triassic evaporitic-carbonate strata. For locations, see Fig. 10b.

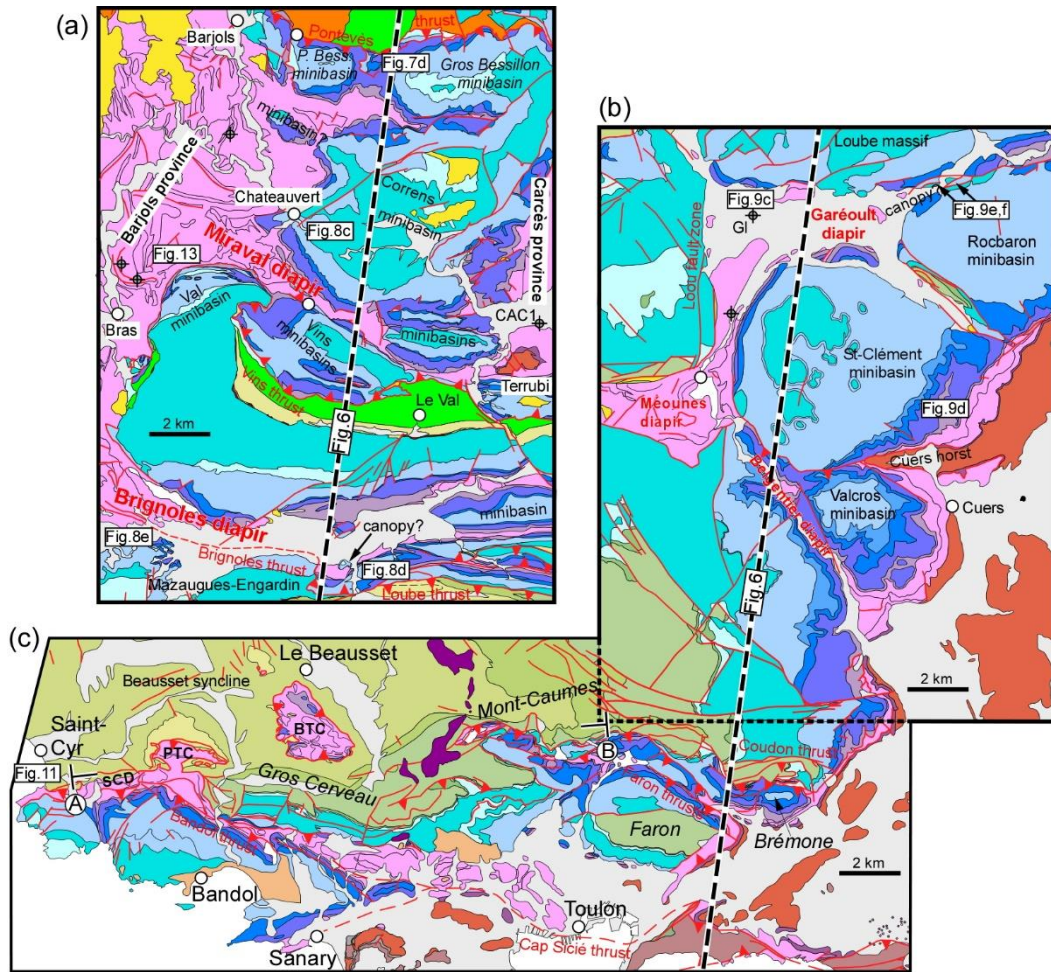


Fig. 10: Zoomed-to three areas on the geological map of Fig. 2 showing salt structures in the eastern Provence fold-thrust belt. (a) Bras imbricate. (b) Loube unit. (c) Coastal inner units. For legend, see Fig. 2. PTC and BTC: Pibarnon and Beausset Triassic coverings, respectively. SCD: Saint-Cyr Triassic doming. A-B: Middle-upper Cretaceous paleogeographic reconstruction of Fig. 14.

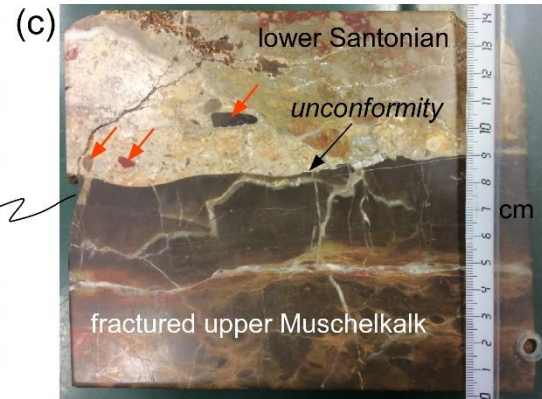
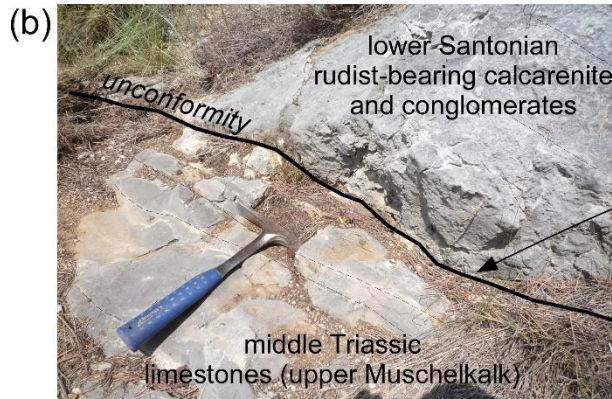
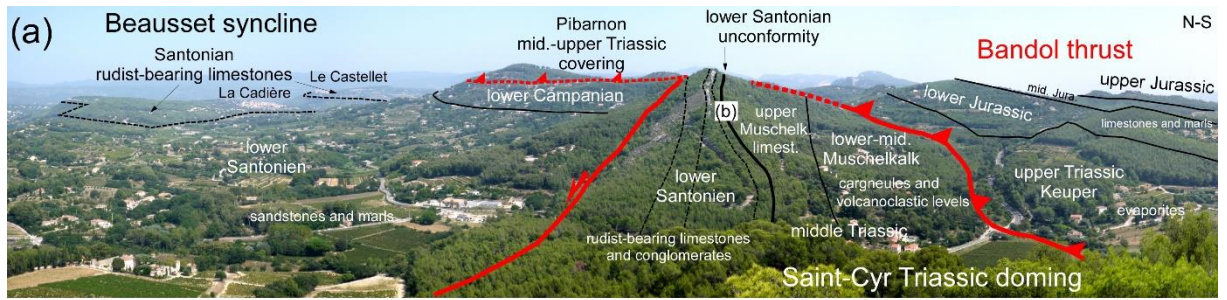


Fig. 11: (a) Panoramic view looking eastward of the Saint-Cyr Triassic doming. For location, see Fig. 10a. In the southern limb of the Beausset syncline, middle Triassic Muschelkalk limestones are unconformably overlain by lower Santonian rudist-bearing limestones and conglomerates. To the south, the dome is overthrust by the Bandol thrust system. (b) Details of the lower Santonian unconformity above Muschelkalk limestones. (c) Zoom of the conspicuous transgressive unconformity surface. Note Triassic upper Muschelkalk pebbles and gravels (red arrows) reworked in the lower Santonian rudist-bearing calcarenite.

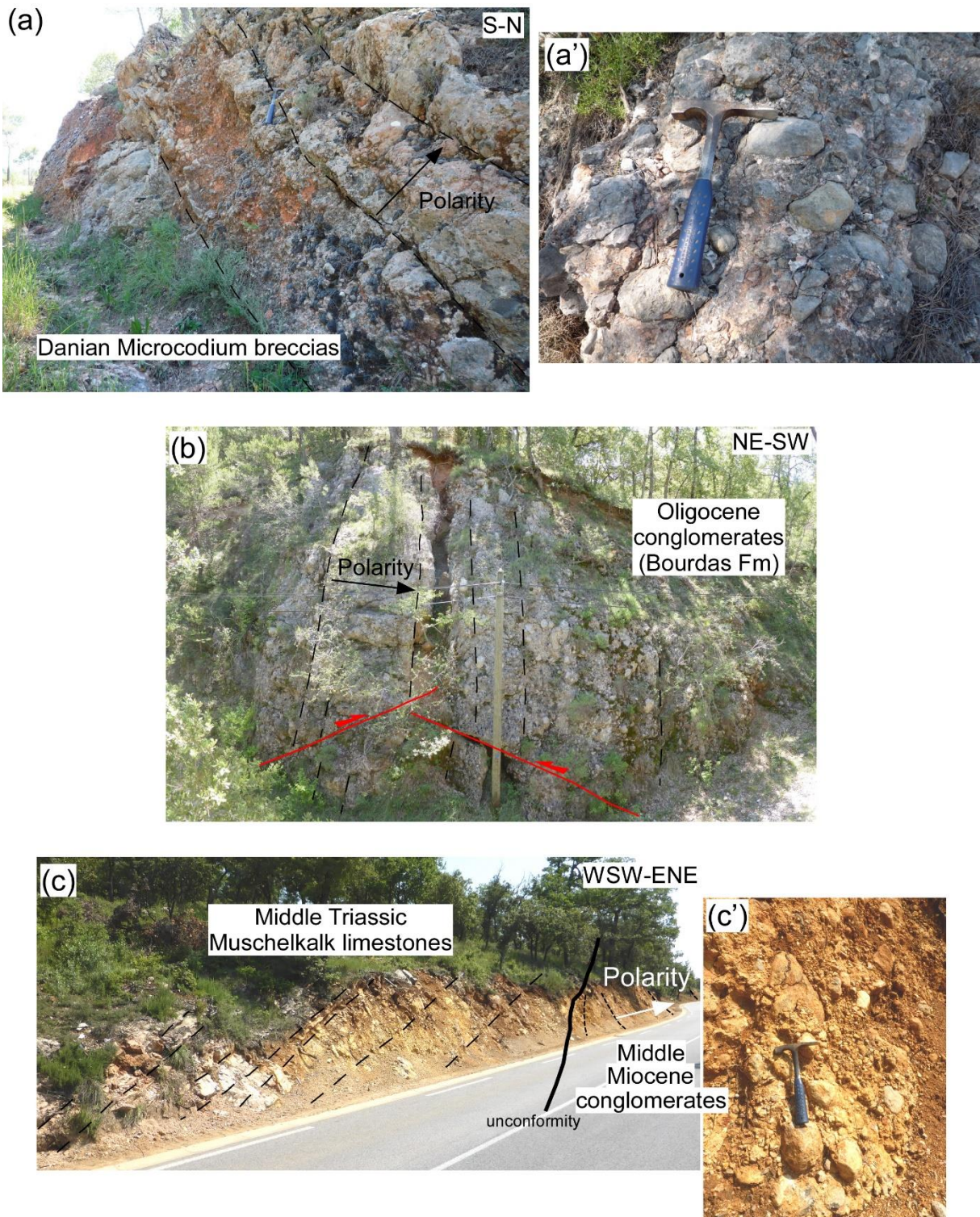


Fig. 12: Evidence for Pyrenean-Provence and Alpine contractional deformations in the eastern Provence fold-thrust belt. For locations, see Fig. 2. (a) Danian syn-tectonic breccia deposits (Microcodium breccias) in the front of the Fox-Amphoux thrust (western edge of the Amphoux syncline). (a') Details of the breccia deposits with pebbles of Jurassic and Cretaceous limestones. (b) Folded and faulted Oligocene conglomerate beds in the northern part of the Barjols Triassic depression (La Combe, east of Rians syncline). (c) Folded middle Miocene conglomerates, sandstones and red shales overlying unconformably middle Triassic Muschelkalk limestones (Brandine, north of Nans town). (c') Details of middle Miocene conglomerates with pebbles of reworked Muschelkalk limestones.

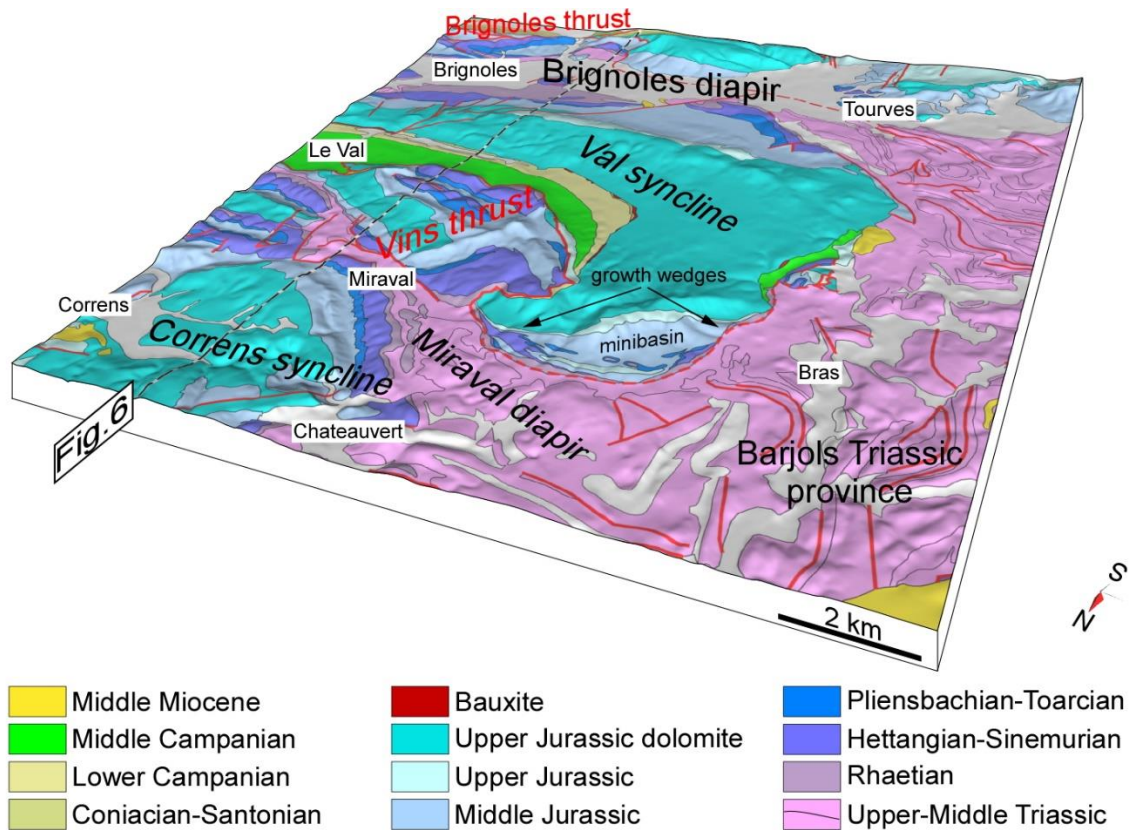


Fig. 13: Three-dimensional diagram of the Bras imbricate. The perspective view looking toward the southeast without vertical exaggeration. The geologic map has been draped on a 25 m resolution digital elevation model. The minibasin geometry of the western edge of Val syncline is shown by growth wedges and unconformities in middle-upper Jurassic strata. The location of the balanced cross section of Fig. 6 is shown.

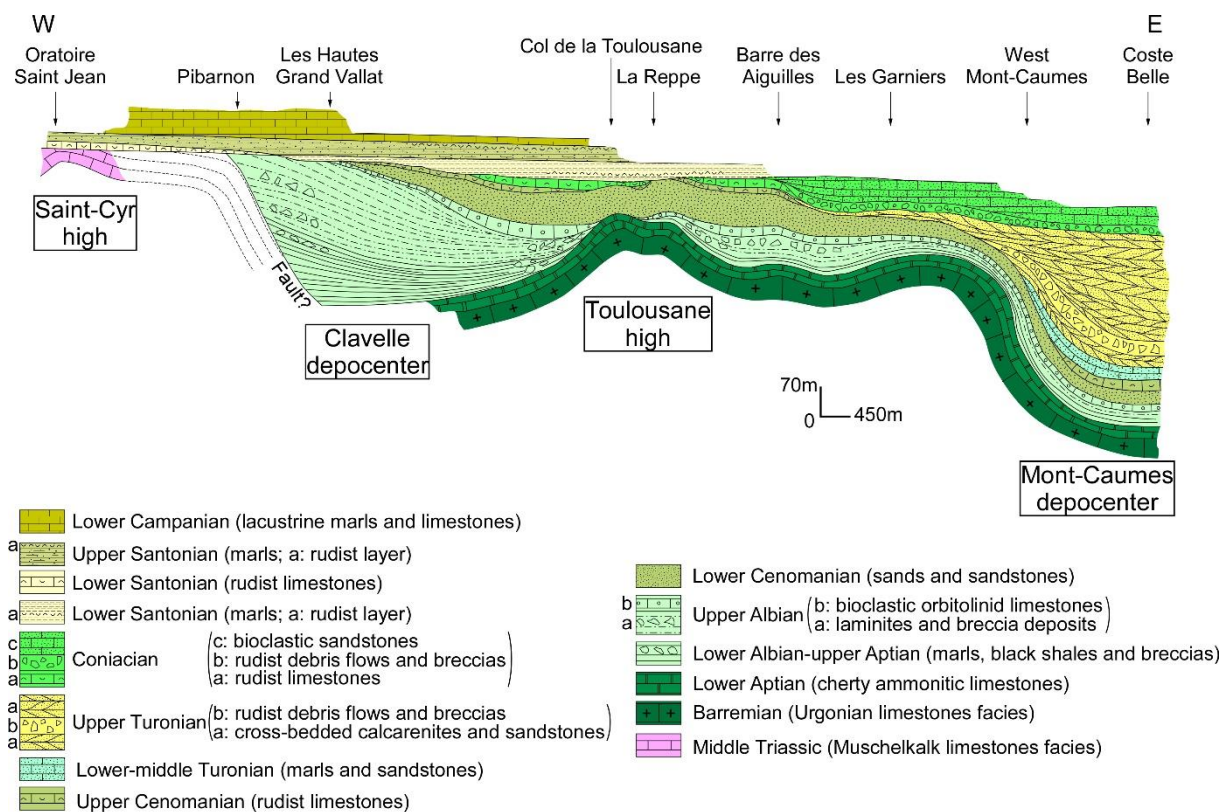


Fig. 14: Updated paleogeographic reconstruction of the southern edge of the Beausset basin during the middle-upper Cretaceous times (after Philip (1970) and Philip et al. (1987), modified). For location, see Fig. 10c.

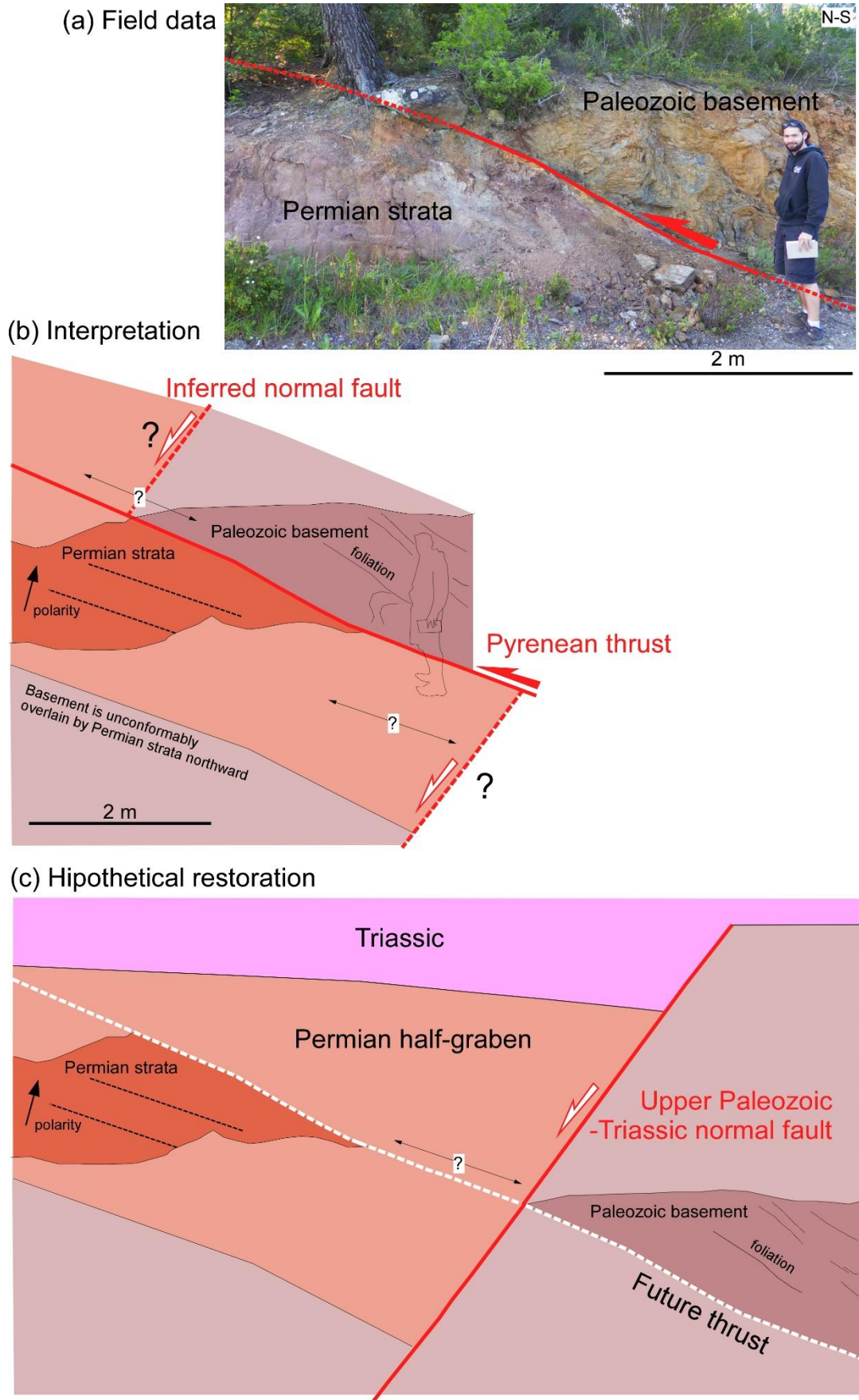


Fig. 15: South-dipping Permian strata overthrust by a north-verging basement thrust in the Maures massif (modified from Bestani et al., 2015). For location, see Fig. 2. Northward, the Permian strata unconformably overlie the basement. We propose that this basement thrust reactivated metamorphic foliation of an inferred basement horst located southward of an upper Carboniferous/Permian-Triassic half-graben. This suggests that the basement thrust propagated with a short-cut behavior through a north-dipping inherited normal fault without structural inversion.

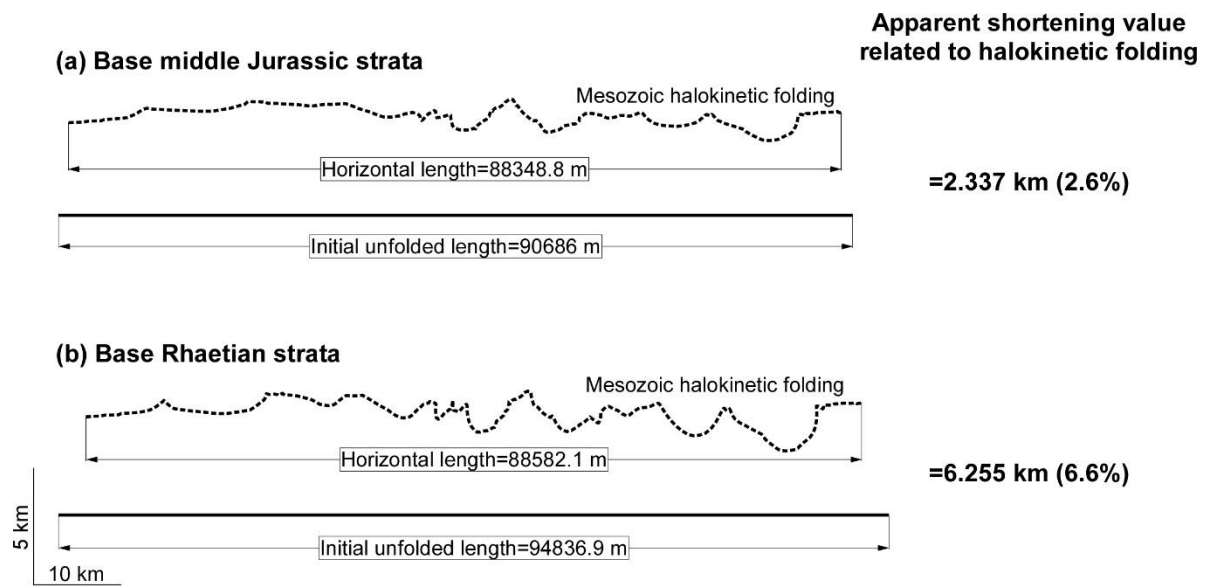


Fig. 16: Quantification of the Mesozoic pre-contractual halokinetic folding. We compare the initial and final horizontal lengths of the (a) middle Jurassic and (b) Rhaetian strata using line-length unfolding. Note the vertical exaggeration.